Université de Sherbrooke

Functional Connectivity in Patients with Brain Tumours

Par
Sukhmanjit Ghumman
Programmes de Science des radiations et imagerie biomédicale

Mémoire présenté à la Faculté de médecine et des sciences de la santé
en vue de l'obtention du grade de maitre ès sciences (M. Sc.)
en Science des radiations et imagerie biomédicale

Sherbrooke, Québec, Canada
Juillet 2017

Membres du jury d'évaluation
Dr. Kevin Whittingstall, département de radiologie diagnostique, FMSS
Dr. M'hamed Bentourkia, département de médecine nucléaire et radiobiologie, FMSS
Dr. Christian Bocti, département de médecine, FMSS

RÉSUMÉ

La connectivité fonctionnelle chez les patients atteints de tumeur cérébrale

Par
Sukhmanjit Ghumman
Programmes de Science des radiations et imagerie biomédicale

Mémoire présenté à la Faculté de médecine et des sciences de la santé en vue de l'obtention du diplôme de maitre ès sciences (M.Sc.) en Science des radiations et imagerie biomédicale, Faculté de médecine et des sciences de la santé, Université de Sherbrooke, Sherbrooke, Québec, Canada, J1H 5N4

Le mode de fonctionement par défaut du cerveau est un réseau cérébral associé à la rêverie et à l'introspection. Des études récentes sur ce réseau ont découvert qu'il est perturbé dans plusieurs pathologies cérébrales. Par example, le mode de fonctionnement par défaut est modulé en démence, TDAH, dépression, schizophrénie et plusieurs autres maladies liés au cerveau. Ceci a mené à l'hypothèse que le mode de fonctionnement par défaut pourrait avoir un rôle dans la physiopathologie des maladies du système nerveux, ou pourrait être un marqueur utile du fonctionnement cérébral. Par contre, très peu d'études ont investigué l'effet de lésions chirurgicaux comme les tumeurs cérébrales sur le mode de fonctionnement par défaut. Par conséquent, le but de ce projet était de caractériser l'importance de l'histologie, de la localisation et de plusieurs autres paramètres de l'effet d'une tumeur cérébrale sur le mode de fonctionnement par défaut.

Mots clés : Glioblastome; Tumeurs cérébrales; Connectivité fonctionnelle; Mode de fonctionnement par défaut

SUMMARY

Functional Connectivity in Patients with Brain Tumours

By
Sukhmanjit Ghumman
Radiation Sciences and biomedical imaging

Thesis presented at the Faculty of medicine and health sciences for the obtention of Master degree diploma maitre ès sciences (M.Sc.) in Radiation sciences and biomedical imaging, Faculty of medicine and health sciences, Université de Sherbrooke, Sherbrooke, Québec, Canada, J1H 5N4

The default mode network of the brain is a set of functionally connected regions associated with introspection and daydreaming. Recent fMRI studies have discovered that the default mode network is often perturbed in the diseased brain. For example, the default mode network is known to be modulated in dementia, ADHD, depression, and schizophrenia, among others. This has led many into believing that this network could have a role in the physiopathology of nervous system disease, or could be a useful marker of brain function. However, very few studies have yet been done which investigate how surgical lesions such as brain tumours affect the default mode network. Consequently, the goal of this project was to characterise the effect of brain tumours on the default mode network based on their location, histological type, and other parameters.

Keywords: Glioblastoma; Brain tumours; Functional connectivity; Default Mode Network

TABLE DES MATIERES

LISTE DES FIGURES

LISTE DES TABLEAUX

Aucun entré de table

LISTE DES ABRÉVIATIONS

BOLD	signal dépendant du niveau d'oxygène sanguin *blood oxygen level dependent*
CBF	flux sanguin cérébral *cerebral blood flow*
DMN	mode de fonctionnement par défaut *default mode network*
ECM	matrice extracellulaire *extracellular matrix*
fMRI	imagerie par résonance magnétique fonctionnelle *functional magnetic resonance imaging*
GBM	glioblastome multiforme *glioblastoma multiforme*
ICA	analyse par composante indépendante *independent component analysis*
LOP	lobe occipito-pariétal gauche *left occipito-parietal lobe*
LTL	lobe temporal gauche *left temporal lobe*
MCC	cortex cingulaire moyen *medial cingulate cortex*
MMP	métalloprotéinase *metalloproteinase*
MRI	imagerie par résonance magnétique *magnetic resonance imaging*
rsfMRI	imagerie par résonance magnétique fonctionnelle au repos *resting state functional magnetic resonance imaging*
SBA	analyse par région d'intérêt *seed based analysis*
PCC	cortex cingulaire postérieur

	posterior cingulate cortex
ROI	région d'intérêt
	region of interest
ROP	lobe occipito-pariétal droite
	right occipito-parietal lobe
RTL	lobe temporal droit
	right temporal lobe

INTRODUCTION

Brain tumours such as glioblastoma multiforme (GBM) are extremely morbid pathologies with poor prognosis. Determining prognosis in patients with brain tumours is a difficult yet very important task, as prognosis can guide treatment. For example, a neuro-oncologist may choose less invasive treatment options for a patient with a brain tumour associated with poor survival, opting rather to maximize his quality of life. In GBM patients, studies have shown that there is a subpopulation of patients who have much longer survival than the average, with some surviving for over 3 years (Johnson, Ma, Buckner, & Hammack, 2012; Scott et al., 1999). Developing modalities that can assist in determining prognosis is important as it would allow physicians to identify these long-term survivors, which could lead to more targeted treatment and better resource management. The broad goal of this master's project was to determine what prognostic information could be extracted from fMRI acquisitions of patients with brain tumours.

We approached this problem by investigating how brain tumours (including GBMs) affected the default mode network, a functional network in the brain associated with various cognitive functions, in a heterogenous group of patients with brain tumours. We also investigated whether characteristics such as location and histology dictated the extent at which the brain tumours affected the default mode network (DMN).

Methods of categorising brain tumours

Intracranial compartment of the tumours

Brain tumours can be categorised by their intracranial compartment. The two main categories which arise from this scheme are "intra-axial" and "extra-axial" tumours. Intra-axial tumours refer to those which are within the brain parenchyma, such as gliomas and metastases. Extra-axial tumours arise from outside the brain, and include meningiomas. An example of an intra-axial and an extra-axial tumour are shown in figure 1.

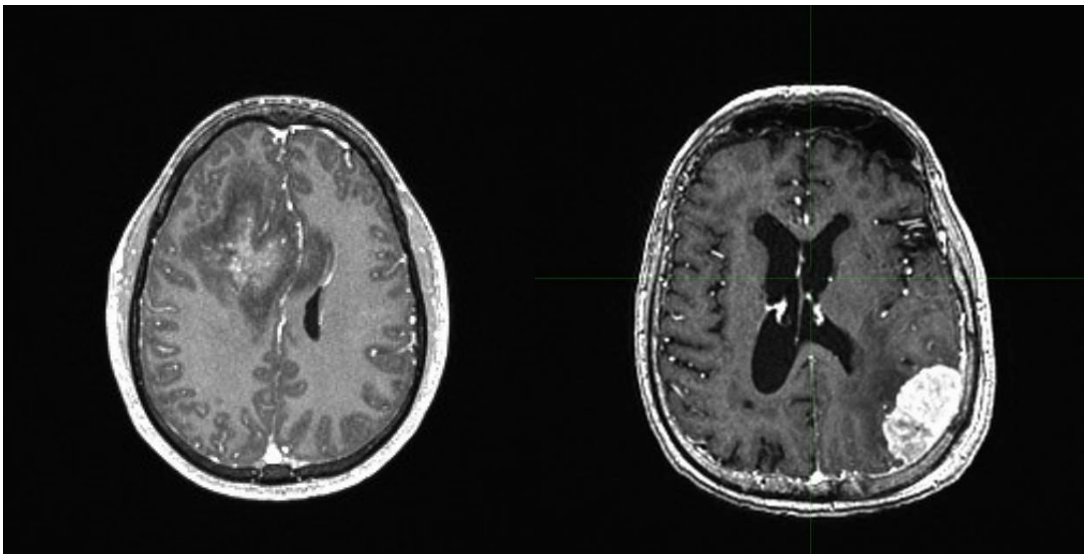

Figure 1 : The difference between intra-axial (left) and extra-axial (right) tumours.

Extra-axial tumours are outside of the brain's parenchyma. For this reason, the brain surface structures, such as gyri and sulci, can be seen at the interface between the tumour and the brain tissue. Another finding demonstrating the extra-axial nature of the tumour on the right is the presence of a meningeal tail, which is a thickening of the meninges around the tumour. This finding argues for a meningeal origin of the tumour.

Histological type of the tumour

The histological type of a tumour refers to its appearance under a microscope. Histology is the classical way of categorising brain tumours, and the WHO's classification of brain tumours, which is the most widely used classification system in neuropathology, is largely based on this parameter (Louis et al., 2016). There exists a very large diversity of histologically distinct brain tumours. Major categories of the most recent revision of the WHO's classification scheme (2016) include gliomas, neuronal tumours, choroid plexus tumours, embryonal tumours, meningiomas, lymphomas and others.

Gliomas

Gliomas are the most common of all primary brain tumours, accounting for 32% of all central nervous system (CNS) brain tumours (Agnihotri et al., 2013). Gliomas are brain tumours arising from the glial cells of the brains. Gliomas are further subdivided based on the type of glial cell which gave rise to the tumour, the main subdivisions including ependymomas, astrocytomas and oligodendrogliomas.

GBM is the grade IV variant of glioma and is the most malignant of all gliomas. It is one of the most morbid cancers to exist with some studies estimating the median survival being as low as 15 months (Thakkar et al., 2014). GBM is a relatively rare condition, with an average incidence rate of 3.19/100000 (Thakkar et al., 2014). Although glioblastoma multiforme is generally a very morbid disease with poor prognosis, there exists a fraction of GBM patients who can survive for longer than 2-3 years (Johnson et al., 2012; Scott et al., 1999). These patients are called long term survivors, and identifying these long-term survivors is a challenge in medicine.

How fMRI works

Conventional MRI

Conventional MRI uses magnetic properties of the hydrogen nucleus to create high-resolution images of the body. Hydrogen nuclei, which have a half integer spin, precess at their Larmor frequency around the static magnetic field (B0) generated by the MRI scanner. Exciting these hydrogen nuclei with an radio-frequency (RF) pulse (B1) leads to a slight amount of them to rotate approximately perpendicular to the direction of the B0 field. While they are in phase, the hydrogen nuclei form a rotating transverse magnetization which can be detected by RF coils.

Once the hydrogen nuclei are perpendicular to the B0 magnetic field, they undergo two processes: longitudinal (T1) and transverse (T2*) relaxation. Longitudinal relaxation,

also named spin-lattice relaxation, is the process by which longitudinal magnetization is re-established after application of an RF pulse. The time required for longitudinal magnetization to reach 2/3 of its maximal value is T1, and this value is a property of the tissue. Transverse relaxation describes the loss of transverse magnetization because of spin-spin interactions in the tissue. These interactions cause the nuclear spins to become out of phase with one another, which leads to a loss of signal. The time required for the transverse magnetization to decay to 1/3 of its maximal value (right after application of the RF pulse) is termed T2, and this value is also a property of the tissue. However, it was noticed experimentally that the true T2 time was much shorter than would be expected from simple spin-spin interactions. In fact, inhomogeneities from the static B0 magnetic field were also found to influence the transverse magnetisation decay rate. The T2* time denotes the decay time when considering spin-spin interactions in addition to field inhomogeneities; it is shorter than the T2 time which only models spin-spin interactions.

These two tissue properties, T1 and T2, are the basis for contrast in MRI. By modulating MRI parameters (echo time or TE and repetition time or TR, amongst others), researchers can enhance tissue with either high T1 (T1 weighted imaging) or high T2 (T2 weighted imaging). Conventional MRI is especially useful for anatomical detail.

BOLD

Neurovascular coupling

Activation of a group of neurons in a certain region of the brain increases energy demands of that region of the brain (Iadecola & Nedergaard, 2007). To avoid a deficit of energy secondary to this increase in energy demand, neural activity is accompanied with an increase in cerebral blood flow. The mechanism which mediates this increase in blood flow secondary to neural activity is called neurovascular coupling (Iadecola, 2004).

Oxyhemoglobin and deoxyhemoglobin

Although neural activity is accompanied with an increase in CBF, it has been shown that this increase in CBF is disproportionately higher than the increase in oxygen consumption caused by the activity (P. T. Fox & Raichle, 1986; P. T. Fox, Raichle, Mintun,

& Dence, 1988). Consequently, areas of neural activity have a decrease in the level of deoxyhemoglobin since an excess of oxygen is being delivered to them (Iadecola, 2004). Oxyhemoglobin is diamagnetic and has similar magnetic properties to surrounding tissues; it does not interfere with the signal generated by surrounding tissue (Gore, 2003). Deoxyhemoglobin, on the other hand, is paramagnetic and has higher magnetic susceptibility than oxyhemoglobin and surrounding tissue. This difference in magnetic susceptibility leads to a distortion of the homogeneity of the B0 magnetic field (see figure 3).

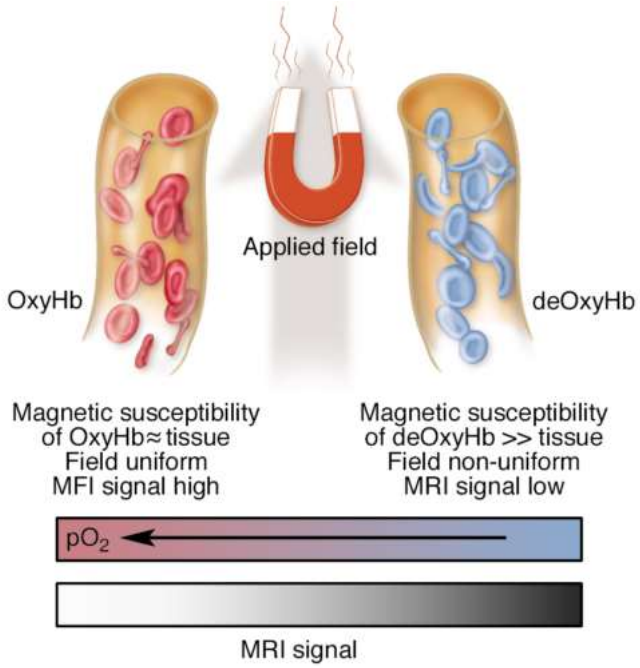

Figure 2: BOLD signal in fMRI

This figure demonstrates the difference in magnetic properties between oxyhemoglobin and deoxyhemoglobin and their impact on the MRI signal.
Reprinted with permission, Journal of Clinical Investigation, (Gore, 2003), copyright 2003

Local magnetic field inhomogeneities disperse the hydrogen nuclei resonant frequencies, consequently accelerating T2 decay and thus accelerating decay of the MRI signal (Gore, 2003; Ogawa, Lee, Kay, & Tank, 1990). Taken all together, neural activity

leads to an increase of the BOLD signal, since neural activity leads to a higher increase in CBF than oxygen consumption.

fMRI applications: resting stage fMRI, functional networks and the DMN

Resting state fMRI

In resting state fMRI (rsfMRI), there is no action performed by the subject in the scanner. The subject is simply asked to stay in the scanner and to avoid thinking. In resting state fMRI, rather than attempting to see how the brain reacts to a stimulus, researchers aim to see how the brain itself is organised, and whether there are related structures within the brain. This is done identifying regions of the brain that have correlated BOLD signals. Such areas are believed to be functional connected and to form functional networks. This method of imaging is ideal for patients with morbid brain pathologies since such patients have difficulty complying with tasks.

Functional networks

Functional networks are areas of the brain with correlated neural activity (Lang, Tomé, Keck, Gorriz-Saez, & Puntonet, 2012; van den Heuvel & Hulshoff Pol, 2010). Examples of these networks include: The Default Mode Network (DMN), the Salience Network and the executive control network. The DMN is illustrated in figure 4. It incorporates the following anatomical areas: the ventral medial prefrontal cortex (vmPFC), the left and right angular gyri (LAG and RAG), the posterior cingulate cortex (PCC) and regions in the temporal lobes.

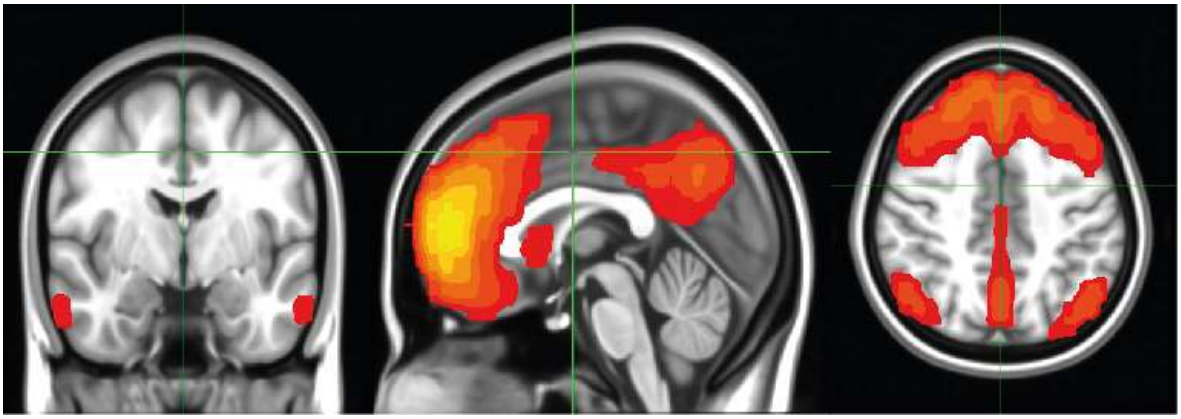

Figure 3 : the default mode network

DMN extracted through independent component analysis (ICA) of a group of subjects. DMN map superposed on a Montreal Neurological Institute (MNI) brain template (from FMRIB software library - FSL).

The default mode network has been extensively studied by scientists, who have shown that it may have a role in daydreaming, planning and introspection (K. C. R. Fox, Spreng, Ellamil, Andrews-Hanna, & Christoff, 2015)

Default Mode Network in the aging brain and various pathologies

Studies comparing the DMN in aging and young subjects have consistently shown substantial decreases in DMN connectivity in the aging brain (Andrews-Hanna et al., 2007; Damoiseaux et al., 2008; Dennis & Thompson, 2014; Hafkemeijer, van der Grond, & Rombouts, 2012; Koch et al., 2010). This decreased functional connectivity affects multiple regions of the brain, including the posterior cingulate cortex (PCC) and the medial prefrontal cortex (mPFC) and has been demonstrated with multiple rsfMRI analysis techniques, including ICA, SBA (seed – based analysis) and graph theory. Data from our own group also corroborates these findings (see figure 5).

Moreover, studies have also shown that the decline in functional connectivity found in the aging brain is correlated to decline in cognitive functions such as memory (Andrews-Hanna et al., 2007). This suggests that rsfMRI and the study of functional networks may be

useful in studying the cause of cognitive decline in the pathological brain. Moreover, it also suggests that brain connectivity may be an indicator of brain disease and may hold information on functional status or prognosis.

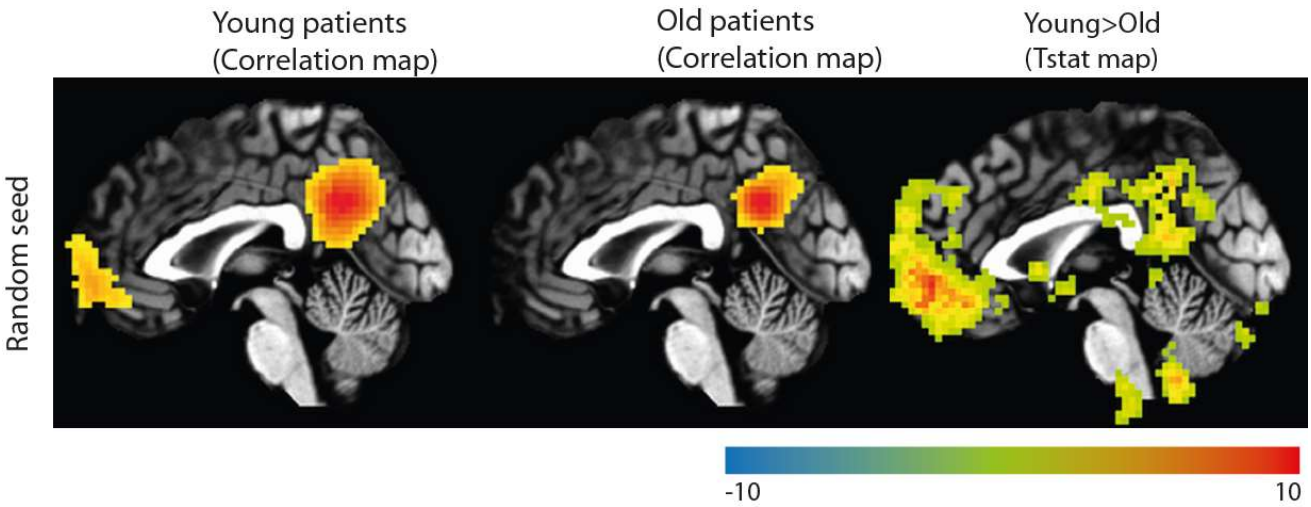

Figure 4 : Age related differences in the DMN

Left : Average DMN correlation map (seed at PCC) of a population of young patients (n=23)
Middle : Average DMN correlation map (seed at PCC) of a population of old patients (n=21)
Right : T-statistic map of the difference between the two populations.

Consequently, researchers have taken a great interest in measuring functional networks in various neuropsychiatric conditions such as autism, schizophrenia, depression, stroke and even brain tumours. The literature on depression serves as a good example to illustrate rsfMRI's potential clinical use in brain pathologies. In fact, researchers investigating functional connectivity in depressed patients have consistently shown a set of changes in the DMN associated with the depressed brain. These changes include increased connectivity within various regions of the DMN (Mulders, van Eijndhoven, Schene, Beckmann, & Tendolkar, 2015). Moreover, they have also shown that these altered functional networks can return to normal after treatment with pharmacological agents (Li et al., 2013) and TMS (Liston et al., 2014), and that these networks can also predict treatment response in depressed patients (Andrew Kozel et al., 2011; Salomons et al., 2014). These

studies thus demonstrate that in depression, and perhaps other diseases, functional connectivity can guide therapeutic decision making and help measure treatment response.

In light of rsfMRI's promising results in depression and other neuropsychiatric conditions, interest grew in investigating functional connectivity in patients with brain tumours. Very few studies have yet been done showing the effect of brain tumours on functional connectivity and on the DMN. These studies tend to demonstrate that the DMN is decreased in patients with brain tumours (see figure 6), although no attempt has yet been made to investigate how location and histology influence this effect. (Esposito et al., 2012; Harris et al., 2014; Maesawa et al., 2015).

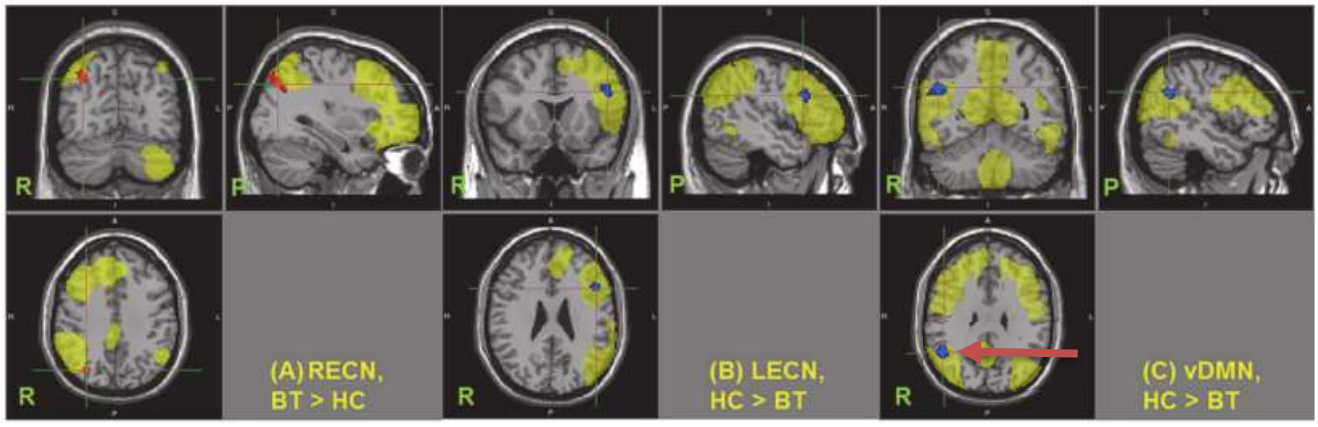

Figure 5 : Altered connectivity in patients with brain tumours

Study showing altered connectivity in patients with brain tumours in three different networks. There was significantly decreased connectivity at the right angular gyrus (red arrow) of the DMN**.**

Source : (Maesawa et al., 2015)**,** PLOS one, open access

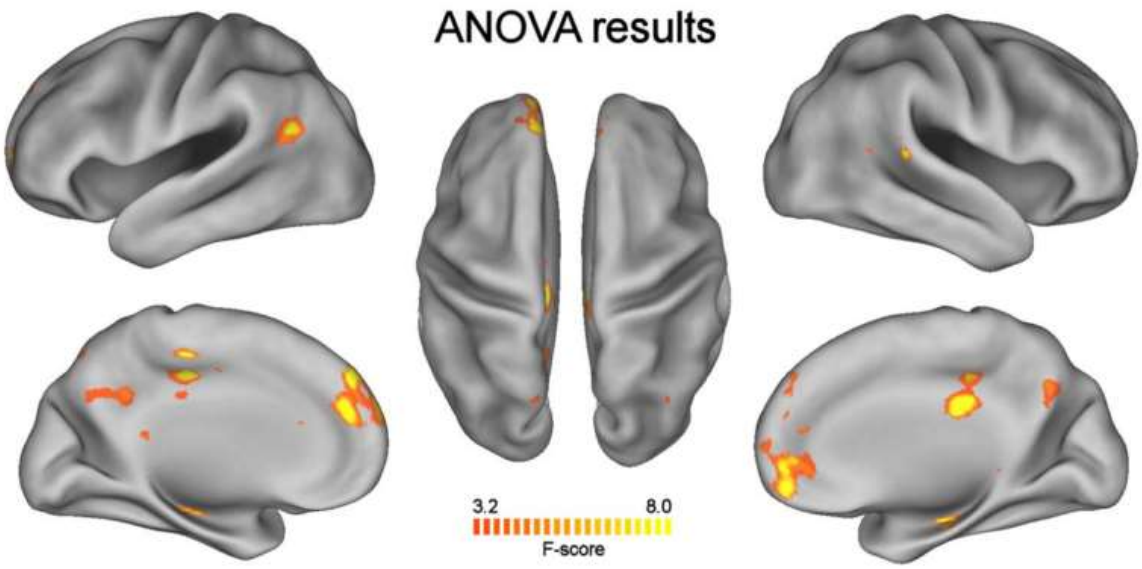

Figure 6: DMN in high and low grade tumours

ANOVA results showing areas where DMN connectivity was significantly different between healthy patients and patients with low and high-grade tumours. Source : (Esposito et al., 2012), PLOS one, open access

How brain tumours can affect fMRI

Migration of glioma cells along white matter tracts

Studies have shown that glioma cells tend to migrate along white matter tracts (Claes, Idema, & Wesseling, 2007). Figure 8 demonstrates this clearly as it shows the presence of glioma cells interspersed along neuronal axons. Glioma cells facilitate their migration by secreting various enzymes such as MMPs (metalloproteinases) (Claes et al., 2007). Metalloproteinases allow the cancer cells to remodel their surrounding extracellular matrix (ECM); changing the ECM leads to a loss of adhesion of the glioma cells and favors migration (Agnihotri et al., 2013; Rao, 2003). In addition to remodelling the ECM, MMPs

could potentially damage surrounding axons as the glioma cells migrate along the white matter tracts and this could lead to perceivable change in fMRI connectivity.

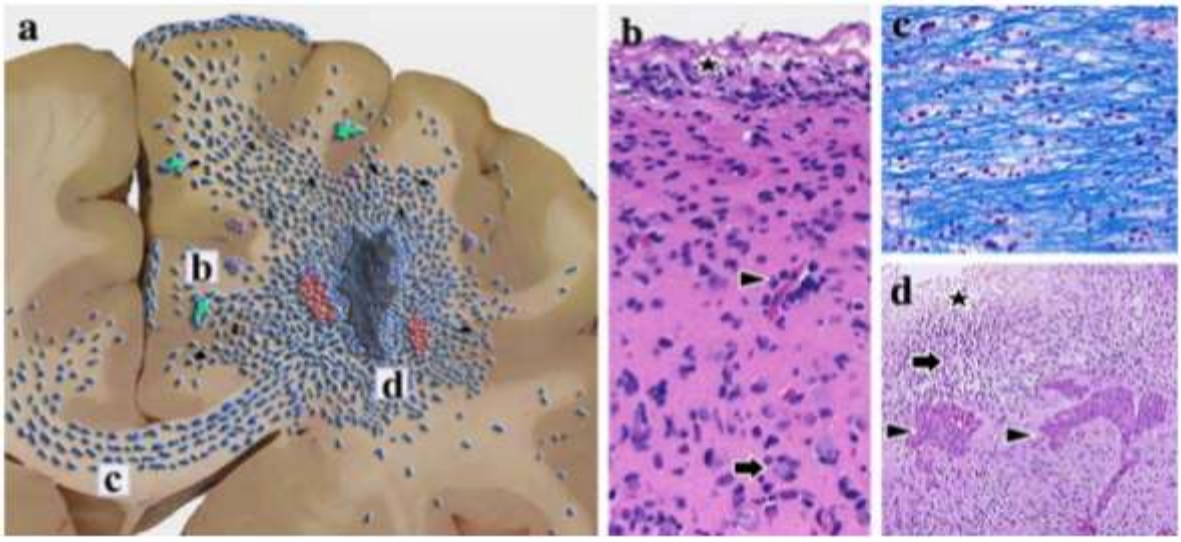

Figure 7: Migration pattern of glioma cells.

Figure shows various migration patterns of glioma cells. A. is a graphical representation of the patterns of migration of gliomas. It demonstrates both the tendency of glioma cells to migrate along white matter tracts and along vessels. B. shows an accumulation of glioma cells around a vessel. C. shows the presence of infiltrating glioma cells within the myelin tracts of the corpus callosum.

Reprinted with permission of Springer, Acta Neuropathologica, (Claes et al., 2007), copyright 2007

Perivascular migration leading to BOLD signal changes

Glioma cells also migrate along vasculature (Claes et al., 2007). The arrowhead in figure 8b. demonstrates an accumulation of glioma cells around a vessel. As previously explained, the fMRI signal is dependent on the ratio of oxyhemoglobin to deoxyhemoglobin, and is consequently highly dependent on vascular properties. Studies have for example demonstrated that the BOLD signal amplitude is correlated to underlying vascular density (Vigneau-roy, Bernier, Descoteaux, & Whittingstall, 2013). Migrating glioma cells could alter properties of nearby vessels such as diameter and consequently alter the fMRI signal. This change in the fMRI signal could lead to a detectable change in connectivity.

Tumours vs strokes of similar size

Functional connectivity studies done on stroke patients have demonstrated decreased in connectivity in various parts of the DMN, including the PCC (Tuladhar et al., 2013). It is worth noting that brain tumours often do not have as large an impact on brain function as do strokes of similar size. This is because brain tumours (including glioblastoma) do not destroy white matter tracts but simply displace them. The slow growth of brain tumours allows the white matter tracts of the brain to be displaced without being damaged, which permits patients with sometimes impressive tumours to maintain a high level of function. In stroke, however, the pathological mechanism is so quick that the brain does not have time to adapt and white matter tracts are consequently interrupted. Thus, brain tumours might be expected to have a much smaller effect on the DMN than do strokes, because the brain has time to adapt to the tumour lesion, and white matter tracts are maintained. This would of course parallel the relative preservation of brain functionality brain tumour patients have when compared to stroke patients.

METHODS

Registration

Before performing the network analysis methods described below, functional and anatomical images are registered/warped to a standardised atlas such as the Montreal Neurological Institute (MNI) atlas. This allows for voxel to voxel statistical comparisons to be made. Without registration, the brains of different individuals would be misaligned, and such statistical comparisons would not be possible.

Seed-based analysis

Seed based analysis (SBA) is the simplest way of performing functional connectivity studies. The method involves placing regions of interest (ROI) in the X nodes of the network being investigated. The BOLD – timeseries falling within each of these regions are averaged together over space, producing X timeseries. Correlation coefficients are then computed between each of these timeseries, which results in an X by X correlation matrix (figure 9). Averaging the unique values of this matrix results in a value representing the investigated network's connectivity. Since the matric is symmetric, each individual network connection is represented twice; therefore, only unique values must be averaged. "Unique values" here means to take either the upper or lower triangle of the matrix.

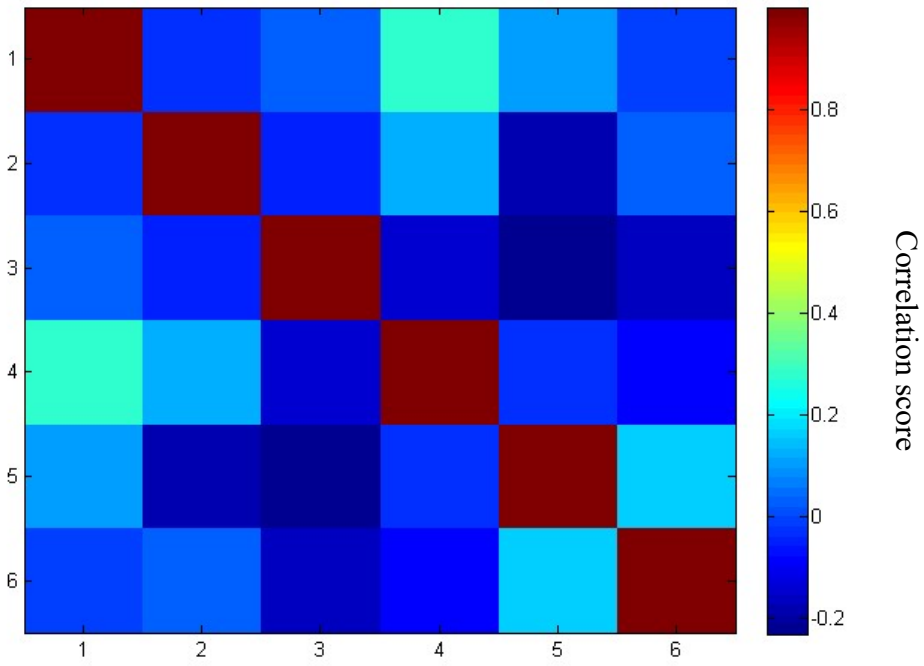

Figure 8 : Example of the correlation matrices which were generated through seed based analysis

Seeds are placed at the 6 DMN nodes and correlation scores are computed between each node and every other node. This produces a 6x6 matrix. Unique values of this matrix can be averaged together to generate a value representing the strength of the default mode network.

SBA can also produce subject specific maps of connectivity. This is done by taking only a single ROI and computing its correlation with every other voxel in the brain (figure 10). This produces a map of correlation coefficients for each subject; these maps can be compared between groups of subjects to identify regional differences in connectivity.

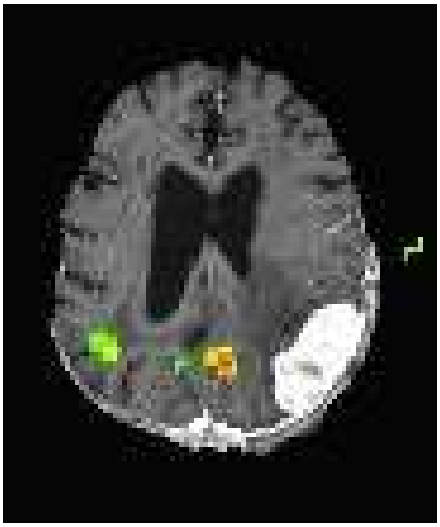

Figure 9 : Example correlation map generated by seed-based analysis

In this example the seed was placed at the PCC. Correlation scores were computed between this seed and every other voxel in the brain. Correlation maps were thresholded to show only significant clusters of voxels. The surviving clusters of voxels represent the default mode network.

Graph theory

Graph theory is a minor extension to traditional seed-based analysis. Rather than placing seeds only on specific network related regions of interest, seeds are placed throughout the brain. The correlation coefficient between each seed and every other seed is computed to build large correlation matrices. Mathematical properties such as density and modularity can then be extracted from these correlation matrices. These properties often have meaningful neural interpretations.

Multi-seed

The multi-seed approach is a method developed by our group to handle the anatomical distortion caused by brain tumours. When brain tumours are located near a DMN node,

traditional SBA cannot be conducted as there is a possibility that the brain tumour causes distortions which displace that DMN node.

An example of this is given in figure 10. This figure demonstrates that placing a seed in the left angular gyrus would lead to erroneous measures of functional connectivity, as the seed would be exactly within a tumour. The seed would be catching tumour tissue rather than brain tissue, which would not generate a correlation map corresponding to the DMN. In less dramatic cases, the seed could still be placed in viable brain tissue, but the tumours proximity to the node may cause a displacement of the DMN node.

The multi-seed approach attempts to solve this issue by first testing several hundred seed locations and picking the best correlated seed with other DMN nodes (figure 11). This seed is presumed to be the true location of the DMN node being investigated. The multi-seed method allows us to model the tumour induced shift of a DMN node.

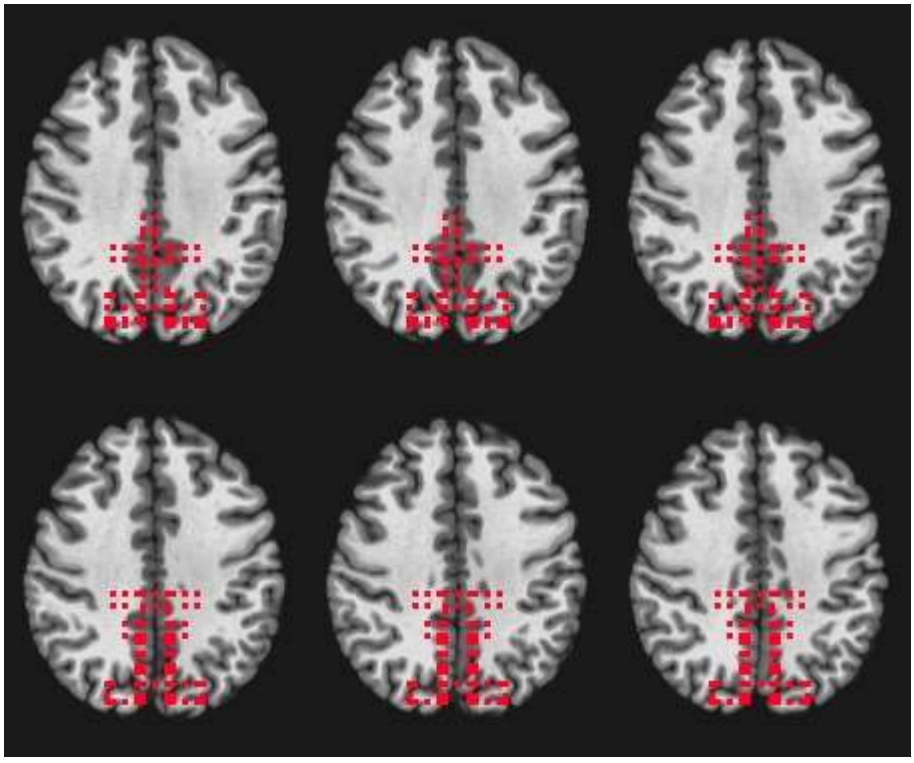

Figure 10 : Multi-seed method

In cases where the brain tumour is located posteriorly in the brain, seeds are placed throughout the posterior cingulate cortex (PCC) area. Correlation maps are generated with each one of these seeds. The seed generating the correlation map most resembling the DMN is taken to be the functional location of the PCC. This method allows to model the tumour's impact on anatomy.

Independent component analysis

Independent component analysis is a model independent method which can extract networks from a group of subjects. The classical explanation of ICA is through the problem it was originally designed to solve, which is named the "cocktail problem". The "cocktail problem" involves a large diner party with several guests during which the host would like to record the conversations of each guest. To accomplish this, the host places as many microphones as there are guests within the room. However, reviewing the recordings afterwards, the host realises that each microphone captured several conversations at the same time, and the individual conversations are consequently not retrievable.

ICA solves this problem as it can extract the different sources of speech from the several recordings. Briefly, the mathematics of ICA involve finding components in the data which are maximally independent and which can linearly be added to reform the initial data. ICA does this by iteratively changing the components until it finds a set of components which have minimal mutual information (mutual information being a metric describes the amount of information we gain about one vector by knowing another). The idea is that each visitor's voice will be poorly correlated with the voices of the other visitors, and should be consequently easy to extract.

ICA is used similarly in fMRI to extract networks. Each network is a voice: it is a set of voxels maximally correlated to each other and minimally correlated to other voxels. The strength of ICA comes from the fact that no prior assumptions toned be made about the networks being investigated. It is model independent, as opposed to SBA, which is model dependent. To perform SBA, the researcher must know the location of the nodes that must

be investigated; consequently, the researcher must have a good reason for investigating those nodes specifically (i.e. must have a clear hypothesis and goal). In ICA, the data is analysed in totality.

Many of ICA's strengths mentioned here are circumvented by the fact that scientists often want to study specific networks anyways. ICA's non-reliance on pre-existing models are consequently not a great advantage for these studies, since a model is being imposed beforehand. For this reason, SBA remains a popular method of performing fMRI research.

ICA's greatest weakness is that it does not consistently produce the same networks from subject to subject. For example, consider figure 12, which are three networks produced by ICA on a subject. By comparing these networks to figure 4, any of these could be the DMN. There is no obvious way of deciding which network is most representative of the DMN. This has hindered ICA's use in group comparisons in fMRI studies. The dual-regression method, discussed next, is an attempt at solving this problem hindering ICA (Filippini et al., 2009).

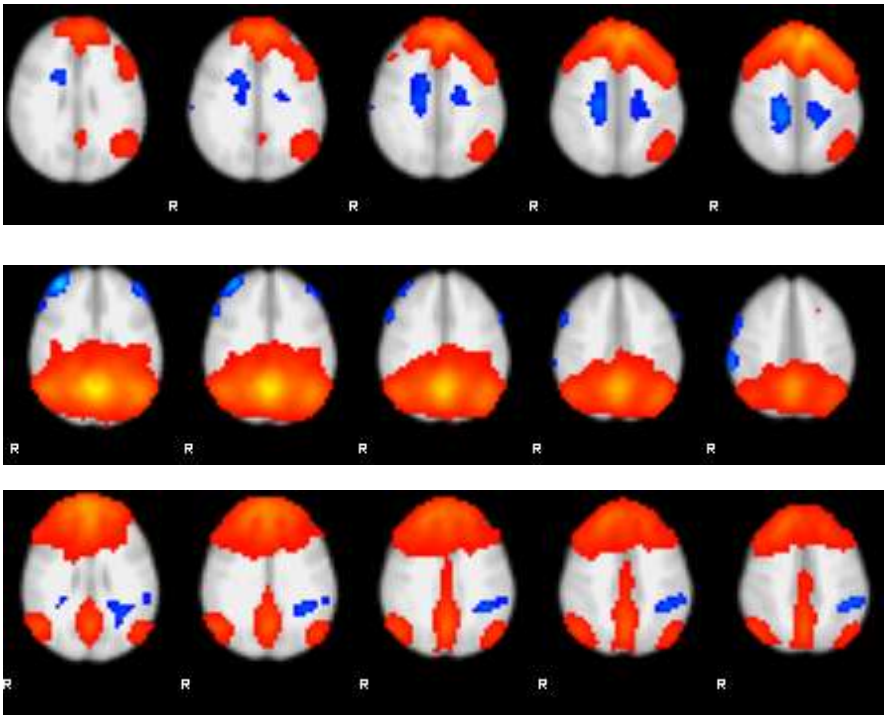

Figure 11 : Example of the output generated by ICA

Three of 25 independent components outputted by ICA. Comparing this figure to figure 4 demonstrates that it is difficult to decide which of these components represent the DMN. Since a similar set of results is produced for each patient, there is no easy way to consistently choose the same components across subjects.

Dual regression

Dual regression is a method of analysing resting state networks which enables ICA to do group comparison studies (Beckmann, Mackay, Filippini, & Smith, 2009; Filippini et al., 2009). ICA does not produce the same ICs for each patient when it is performed on a subject to subject basis. Consequently, there is no easy way of consistently choosing the right components (DMN related components) across subjects. Dual regression solves this by performing group ICA rather than subject to subject ICA. This is done by concatenating all the fMRI datasets across time and performing ICA on this large 4d dataset. The DMN is then identified visually by parsing through the components. This chosen DMN map is used as a spatial regressor in each subject to extract DMN-related subject-specific timeseries, which

are then used as a temporal regressors to extract subject-specific DMN maps. This method is superior to traditional subject to subject ICA as the decision on choosing which components represent the DMN is only made once (on the group ICA results).

ARTICLE 1

Exploratory study of the effect of brain tumors on the default mode network

Auteurs de l'article: Sukhmanjit Ghumman, David Fortin, Maxime Noel-Lamy, Stephen C. Cunnane, Kevin Whittingstall

Statut de l'article: publié dans Journal of Neuro-Oncology (2016)

Avant-propos: Je suis la personne qui a réalisé les analyses statistiques et qui a rédigé cet article, avec l'aide de K. Whittingstall. Les acquisitions des sujets sains ont été faits par S.C. Cunnane et M. Noel-Lamy. Les acquisitions des patients atteints de tumeurs ont été faits par D. Fortin. D. Fortin était aussi disponible comme source de connaissance sur les tumeurs cérébrales.

Résumé : L'IRMf fait à l'état de repos est une méthode populaire pour visualiser les réseaux fonctionnels du cerveau. Un de ces réseaux, appelé le mode de fonctionnement par défaut, est altéré dans plusieurs états pathologiques, dont les tumeurs cérébrales. Par contre, très peu d'études ont tenté de trouver un lien entre la localisation des tumeurs et leur type histologique et l'impact qu'ils ont sur le mode de fonctionnement par défaut. On a collecté des données de l'IRMf chez 73 patients atteints de tumeurs cérébrales pour évaluer l'effet que ces tumeurs ont sur le mode de fonctionnement par défaut selon la localisation, la taille et l'histologie de la tumeur. Ceci a été fait en comparant les patients atteints de tumeur à des contrôles sains en utilisant l'analyse en composantes indépendantes et l'analyse par définition de régions d'intérêt. Nous avons trouvé que les tumeurs se localisant au niveau de l'hémisphère gauche avaient le plus grand impact sur le mode de fonctionnement par défaut tandis que les tumeurs dans l'hémisphère droite n'avaient pas d'effets.

J Neurooncol (2016) 128:437–444
DOI 10.1007/s11060-016-2129-6

CLINICAL STUDY

Exploratory study of the effect of brain tumors on the default mode network

Sukhmanjit Ghumman[1] · D. Fortin[2] · M. Noel-Lamy[4] · S. C. Cunnane[3] · K. Whittingstall[1,4]

Received: 27 January 2016 / Accepted: 7 April 2016 / Published online: 18 April 2016

Abstract Resting state functional magnetic resonance imaging (RS-fMRI) is a popular method of visualizing functional networks in the brain. One of these networks, the default mode network (DMN), has exhibited altered connectivity in a variety of pathological states, including brain tumors. However, very few studies have attempted to link the effect of tumor localization, type and size on DMN connectivity. We collected RS-fMRI data in 73 patients with various brain tumors and attempted to characterize the different effects these tumors had on DMN connectivity based on their location, type and size. This was done by comparing the tumor patients with healthy controls using independent component analysis (ICA) and seed based analysis. We also used a multi-seed approach described in the paper to account for anatomy distortion in the tumor patients. We found that tumors in the left hemisphere had the largest effect on DMN connectivity regardless of their size and type, while this effect was not observed for right hemispheric tumors. Tumors in the cerebellum also had statistically significant effects on DMN connectivity. These results suggest that DMN connectivity in the left side of the brain may be more fragile to insults by lesions.

Keywords Default mode network · Glioma · Functional connectivity · Posterior cingulate cortex · fMRI

✉ K. Whittingstall
kevin.whittingstall@usherbrooke.ca

[1] Departments of Nuclear Medicine and Radiobiology, Faculty of Medicine and Health Science, Université de Sherbrooke, 12e Avenue Nord, Sherbrooke, QC, Canada

[2] Department of Surgery, Faculty of Medicine and Health Science, Université de Sherbrooke, 12e Avenue Nord, Sherbrooke, QC J1H 5N4, Canada

[3] Department of Medicine, Faculty of Medicine and Health Science, Université de Sherbrooke, 12e Avenue Nord, Sherbrooke, QC J1H 5N4, Canada

[4] Present Address: Department of Diagnostic Radiology, Faculty of Medicine and Health Science, Université de Sherbrooke, 12e Avenue Nord, Sherbrooke, QC J1H 5N4, Canada

Introduction

Functional magnetic resonance imaging (fMRI) using the blood oxygen level dependent (BOLD) signal has provided a method of non-invasively inferring brain activity in humans. Recent discovery of low frequency temporally correlated BOLD signals in spatially distant parts of the brain at rest has provided evidence for the existence of functional networks within the brain. Amongst these networks, the so called default mode network (DMN), a resting state network, has gained particular attention from researchers [1, 2]. Patients with schizophrenia, autism and dementia have exhibited altered connectivity in the DMN [3]. Studies done on brain tumor and stroke patients have also shown alterations of the DMN [4–7], and one study associated DMN connectivity strength to various neuropsychometric performance scores [4]. Despite the growing body of work relating DMN connectivity to neurological disorders, few studies have attempted to determine the effect of brain lesion localization and type on activity in the DMN. However, such studies could potentially identify subcortical and cortical brain areas important for DMN integrity. Moreover, such studies could also lead to the discovery of a pathophysiological role of the DMN in the symptomatology of brain tumors, and could be of benefit to clinicians in the field of neuro-oncology when

they consider whether a patient is likely to benefit from surgery and subsequent adjuvant treatment.

We therefore collected BOLD data in 73 patients with different types of tumors in order to study the effect of tumor location, type and size on the DMN. DMN integrity was evaluated using a seed-based correlation approach and with independent component analysis (ICA).

Materials and methods

Scanning procedures

This study was approved by the research center's ethics committee, and written consent was acquired from all patients. High resolution T1 weighted MPRAGE anatomical scans were obtained at the Centre de recherche du Centre hospitalier de l'Université de Sherbrooke on a Siemens 1.5 T MR scanner. 73 patients with brain tumors were enrolled. Anatomical resolution of the scans was $1 \times 1 \times 1$ mm. Functional BOLD scans were obtained on the same machine at a resolution of $3.75 \times 3.75 \times 3.00$ mm and TR/TE(repetition time and echo time) of 3.864/0.04 s. Control subjects ($n = 23$) were also recruited for this study; scanning parameters and experimental protocol were the same. Each tumor was manually segmented using MRIcron software [8]. Tumor patients had an average age of 56.4 (standard deviation: 14.5) whereas control subjects had an average age of 73.4 (standard deviation: 5.7). The default mode network is known to be more correlated in younger patients [9]. We consequently only investigated decreases in DMN, which would consequently not increase the rate of false positive results (at the expense, however, of more false negatives).

fMRI data pre-processing

Preprocessing of anatomical and functional data was done with the AFNI software package [10, 11] using a modified pre-processing pipeline generated by the uber_subject.py script. Briefly, anatomical datasets were skull-stripped and warped to the Montreal Neurological Institute (MNI) standardized space with a linear transformation. Functional data was despiked, slice time-corrected, coregistered to MNI template, and blurred with a 4 mm Gaussian kernel. Quality of coregistration was inspected visually by comparing alignment of several anatomical structures, including the genu and splenium of the corpus callosum, the lateral ventricles, and the occipital and frontal poles. Motion correction was done with a rigid body transformation. Time points where movement exceeded 0.4 mm were discarded. The time series were then bandpass-filtered between 0.01 and 0.1 Hz [12]. Cerebrospinal fluid and white matter were also regressed out of the signal by first segmenting the brain into tissue-based categories and adding the mean time series within each mask to a general linear model (GLM).The resulting datasets were used for seed-based analysis and dual regression analysis (see below).

Identification of default mode network nodes

Independent component analysis (ICA) with FSL's MELODIC software [13] was performed on all the subjects in order to create a group wide spatial map of the DMN. This map served two purposes: to identify coordinates of the major DMN nodes for seed placement in the seed-based analysis and to serve as a spatial regressor in the first step of the dual regression analysis.

MELODIC-ICA was performed using a temporal concatenation approach: group-wide independent components were estimated from the concatenated pre-processed functional datasets of the patients. ICA was programmed to extract 25 independent components in accordance with previous studies [14]. DMN related components were identified by measuring the correlation between these components and the reported DMN found by Shirer et al. [15] (available at: http://findlab.stanford.edu/functional_ROIs.html); the component with the highest correlation was taken to be the DMN. Coordinates of the peak intensities of six known DMN nodes (ventral medial prefrontal cortex, bilateral inferior parietal areas, medial temporal gyri, posterior cingulate cortex) were noted for seed based analysis.

Seed-based analysis (SBA)

In all patients, 5 mm spheres were placed at the DMN coordinates determined previously and the average time series at each of these seeds was extracted. Correlation coefficients between these time series were computed and converted into Z-scores using Fisher's transformation. Since six DMN nodes were studied, this produced 15 unique Z-scores per patient, which were then averaged together for each patient to produce a measure of overall DMN connectivity. One way ANOVA tests were performed with tumor type and location as grouping variables to determine if there was any significant difference in overall DMN connectivity across either of these variables. For further analysis, ANOVA was also done with tumor lesions grouped as either intra-axial or extra-axial (glial lesions, lymphomas, metastasis vs meningiomas and cysts), and infiltrative or non-infiltrative (glial vs all other diagnoses). Moreover, we also studied the effect of tumor size on overall connectivity with a simple regression analysis.

Dual-regression analysis

As was mentioned earlier, anatomy distortion is expected to be a significant confound in the seed based analyses. Tumor induced DMN node shift could lead to misplaced seeds and consequently decreased correlation scores without there being any underlying decrease in DMN connectivity. This motivated the use of group ICA coupled with subject back projection using the recently developed dual regression method [16]. Briefly, the group DMN spatial component estimated from ICA was used in a regression analysis in order to extract DMN related "timecourses" for each patient; these time courses were then used in a second regression analysis to determine independent component (IC) maps for each individual. Essentially, this is a form of seed-based analysis where the seed is larger and incorporates all DMN areas at the same time [17]; it is potentially less sensitive to distorted anatomy than the correlation analysis since "seeds" are larger and data-derived. This methodology was used to infer long distance decreases in connectivity (decreases in connectivity far from tumor location); such decreases cannot be imputed on local anatomy deformation from the tumors. Comparisons between groups was done with non-parametric permutation tests (5000 permutations) [18, 19]. We used a cluster mass-based method implemented in FSL to control family wise error rate to less than 0.05. Only DMN areas were evaluated by permutation testing (by using a mask) in order facilitate computation and to increase power of the study. One-tailed tests were performed, so only decreases in DMN connectivity were investigated. This is in accordance to the previous studies done on tumor patients, which usually find decreases in DMN connectivity [4, 5, 20]. In addition, as explained previously, only decreases in DMN connectivity would be easily interpretable, because of the age mismatch of our cohorts.

Results

Of the 73 patients, one did not pass through the GLM step because of excessive motion, leading to an insufficient number of time points to estimate all necessary parameters. Another had heavily distorted brain anatomy and coregistration failed. These two patients were excluded from the rest of the study.

Tumors were subdivided into seven subgroups depending on their anatomic location in the brain, in an effort to study the effect of their localization on DMN connectivity. Frontal lobe, left and right occipito-parietal lobes(LOP and ROP), left and right temporal lobes (including areas directly above the sylvian fissure) and subtentorial were chosen as anatomical subgroups. Tumors near the medial cingulate cortex (MCC) were also chosen as another subgroup despite small sample size ($n = 6$) because of the cingulum's believed importance in DMN connectivity. Four patients had tumors near the midbrain and were excluded from the rest of the study. Histological diagnoses of the remaining patients are summarized in Table 1.

ANOVA yielded no significant differences in overall connectivity scores between patients with different types of tumors ($p = 0.4911$) or with tumors located in different areas of the brain ($p = 0.1179$).We also carried 2 different analyses (one way ANOVA) using groupings based on intra-axial vs extra-axial tumor, and infiltrative vs non-infiltrative tumors: neither of these analyses showed significant difference in their impact on DMN ($p = 0.7352$ and $p = 0.4029$ respectively).

However, these analyses were heavily biased by the anatomy distorting effect of tumors. In other words, tumors may have deformed the brain's architecture to the point of displacing DMN nodes, in which case seed based analysis would miss these nodes. For this reason, we used ICA coupled with dual regression, which is potentially less impacted by this effect.

Results of group comparisons with dual regression are summarized in Fig. 1 and in Table 2. These analyses investigated the effect of tumor location. Our dataset was not large enough to control for both tumor location and tumor type (Table 1). No significant differences were found between control and patients with mass lesions in the right temporal lobe, right occipito-parietal lobe or MCC ($p > 0.05$). Patients with tumors in the left temporal lobe had a statistically significant decrease of DMN connectivity at the left angular gyrus ($p = 0.022$), and patients with tumors in the left occipito-parietal lobe had significant decrease at both left angular gyrus (LAG) and posterior cingulate cortex (PCC) ($p = 0.001$). Patients with cerebellar tumors had significantly reduced DMN connectivity at medial prefrontal cortex (mPFC) ($p = 0.038$). Patients with tumors in the frontal lobe had nearly significant decreases at PCC ($p = 0.117$) and mPFC ($p = 0.129$). In summary, these results suggest that some left–right asymmetry may exist in the effect tumors have on the default mode network. In fact, left sided tumors seem to have a larger effect on DMN connectivity.

Caveat on the anatomy distorting effect of tumors

As can be seen in Fig. 1, tumors located in the cerebellum and left temporal lobe suppress connectivity in distant cortical regions. In tumors near the LOP, however, the decrease in PCC connectivity reported is near the location where the tumors are. This makes it difficult to interpret the result, since it is possible that the tumors simply displaced the PCC node. In this situation, DMN connectivity may

Table 1 Diagnosis of patients and localization of tumours

Pathological diagnosis	Glial lesion	Metastatic tumour	Meningioma	Other	Total
Anatomical subgroups					
Tumour at frontal lobe	10	1	1	2	14
Tumour at LOP	6	1	1	0	8
Tumour at ROP	8	2	3	1	14
Tumour at MCC	3	2	0	1	6
Tumour at left temporal lobe	5	3	2	0	10
Tumour at right temporal lobe	6	2	0	0	8
Tumour at cerebellum	2	1	1	3	7
Total	40	12	8	7	67

actually be unaffected, and the difference might simply reflect PCC node displacement. To investigate this effect, we attempted to locate the PCC node in each patient by finding the region in the PCC which showed highest correlation to DMN areas (right angular gyrus, mPFC and the medial temporal gyri). This was done with a multi-seed approach: we placed 382 equidistant 5 mm seeds in various locations of the PCC and precuneus and created correlation maps. For each of these 382 seeds, we averaged the correlation scores over a mask to identify the seed that showed the highest correlation to the DMN nodes. The (x, y, z) coordinates of this "best" seed was averaged in the healthy controls and the tumor patients to see whether the PCC node was deviated. The results of this are shown in Fig. 2. This figure clearly demonstrates that LOP tumors did indeed significantly push the PCC node towards the right, and the difference in PCC connectivity shown with the dual regression method is likely due to this displacement. Figure 2b, c, which are average correlation maps of LOP tumor patients and healthy subjects (using the "best" seed) also show the PCC displacement.

To see whether the LOP tumors had an effect on DMN connectivity (and not just DMN location), we pooled the 10 "best" seeds (i.e. 10 seeds which showed the highest correlation to other DMN areas) for each patient and healthy subject. We used these seeds to create correlation maps and averaged the correlation scores over the DMN mask previously described (which excludes areas near the tumors). We then tested for differences in PCC connectivity to the masked DMN regions in healthy subjects and patients with tumors in LOP and ROP (control) with a Student's *t* test. We found that LOP tumors still had an effect on DMN connectivity, and this effect was statistically significant when compared to healthy patients ($p = 0.0028$) whereas ROP tumors did not have a statistically significant effect ($p = 0.4848$). Over concerns of the normality of the data, we also compared the three groups with Mann–Whitney U tests and non-parametric permutations tests (10,000 permutations) and these tests yielded similar results. The results of the non-parametric permutation tests are shown in Fig. 2 d); the Mann–Whitney test found significant difference between LOP tumor patients and healthy patients (healthy > LOP, $p = 0.0066$) but none between healthy patients and ROP tumor patients ($p = 0.6131$). These results shows that LOP tumors do indeed have a disproportionate effect on DMN connectivity (when compared to ROP tumors), and this effect persists when we take into account the tumors' effect on PCC node location.

The effect of cerebellar tumors on mPFC connectivity and of left temporal tumors on LAG (found with dual regression) cannot be attributed to anatomy distortion, since in these cases the areas affected by tumor and the DMN regions showing difference in connectivity were not close to each other.

Discussion

Table 3 summarizes our findings. Briefly, we demonstrated that tumors in the left side of the brain significantly decreased connectivity of the DMN, an effect that was not present for right sided tumors. Moreover, our multi-seed approach showed that the tumors could displace the DMN nodes when the two are in proximity to each other.

In light of these results, we have come to several conclusions regarding functional connectivity in tumor patients. First, we find that blind seed based correlation studies are inappropriate in tumor patients, because of the confounding effect of anatomy distortion. We propose that any type of correlation study done with tumor patients should pool these patients based on the location of their tumor, in order to be able to evaluate the effect the tumors had on DMN node locations. Knowledge of tumor location and how they might displace DMN nodes is critical when attempting to interpret results of statistical testing, as was shown in this paper. Anatomy distortion can be accounted

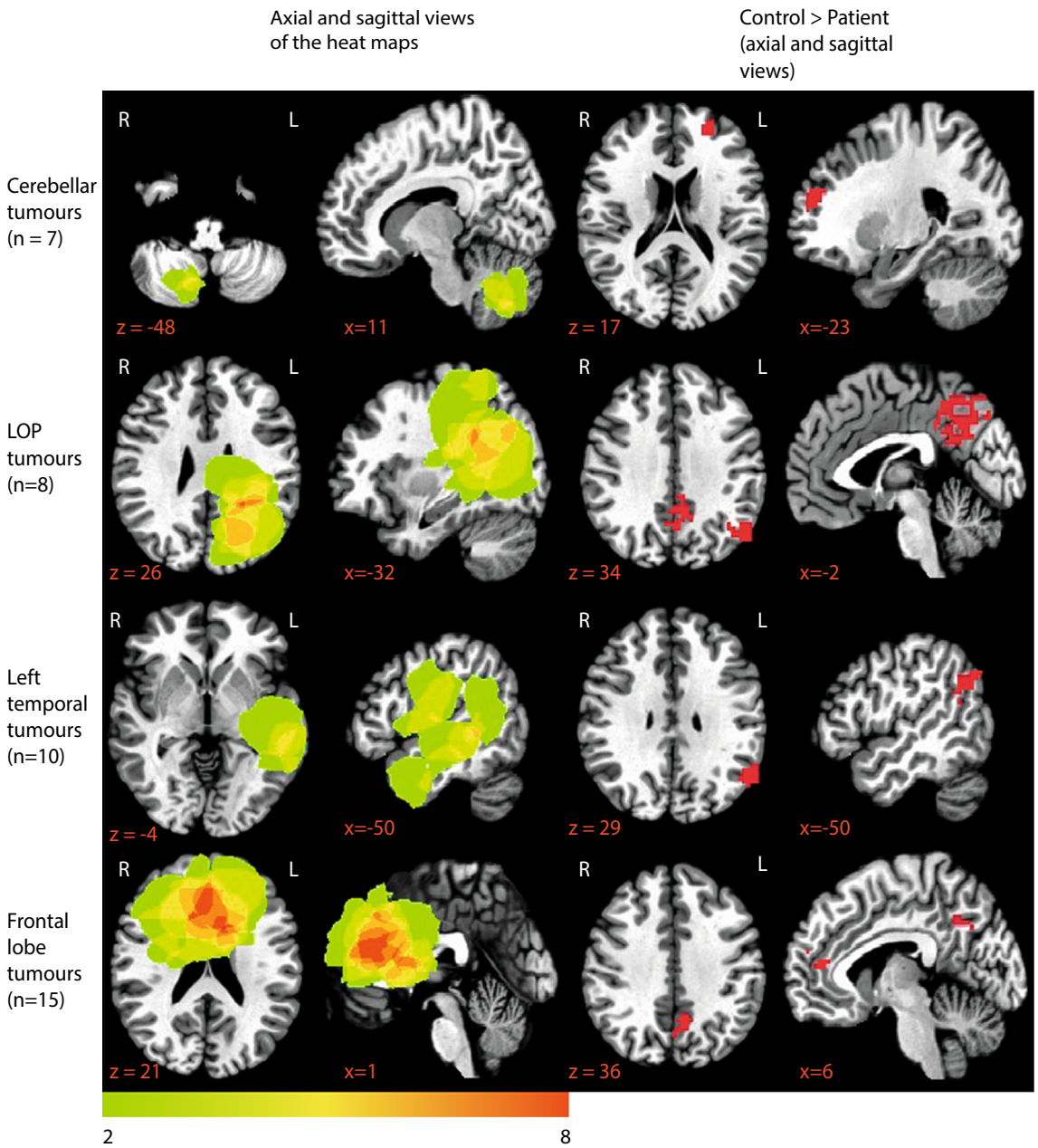

Fig. 1 *Each row* is one of the subgroups that were largely different from control. The *first three* represent patients with tumors in the cerebellum, left temporal lobe and left occipito-parietal lobe, which were the only subgroups with statistically significant differences. The *last row* represents the subgroup of patients with tumors in the frontal lobe, whose connectivity differed largely from control, although this was not significant. *First two columns* are heat maps of the tumors for each subgroup, whereas the *last two columns* show statistically significant clusters of the contrast between control and each subgroup

for with the multi-seed approach we have used in this paper, where the seed showing highest correlation to other DMN nodes is taken for comparisons between healthy and tumor patients. We recommend this multi-seed approach for any situation where DMN nodes may be displaced (strokes, cortical atrophy, concussions, etc.).

In terms of the anatomical location of the tumors, we found some left–right asymmetry in the DMN's ability to resist lesions. In fact, left sided tumors tend to have a larger effect on DMN connectivity than right sided tumors. Moreover, tumors in the LOP lobe had a particularly important effect on the DMN, causing both decreased connectivity at PCC nodes and displacing the PCC node from its location in healthy patients. The decreased PCC connectivity persisted when taking into account anatomical distortion: the PCC seeds showing highest correlation (the "best" seeds) to other DMN nodes had lower correlation scores in LOP tumor patients than in healthy patients. ROP

Table 2 Clusters

Contrast	Anatomical position	Number of voxels	p value
Control > $\text{Patient}_{\text{Cerebellum}}$	Prefrontal cortex	46	p = 0.038*
Control > $\text{Patient}_{\text{LOP}}$	Posterior cingulate cortex	216	p = 0.001*
Control > $\text{Patient}_{\text{LOP}}$	Left angular gyrus	69	p = 0.025*
Control > $\text{Patient}_{\text{Left temporal}}$	Left angular gyrus	79	p = 0.022*
Control > $\text{Patient}_{\text{Frontal}}$	Prefrontal cortex	34	p = 0.129
Control > $\text{Patient}_{\text{Frontal}}$	Posterior cingulate cortex	34	p = 0.117

* These p values remained significant after an FDR correction with $q < 0.10$ using the Benjamini and Hochberg procedure with $m = 7$ (seven comparisons)

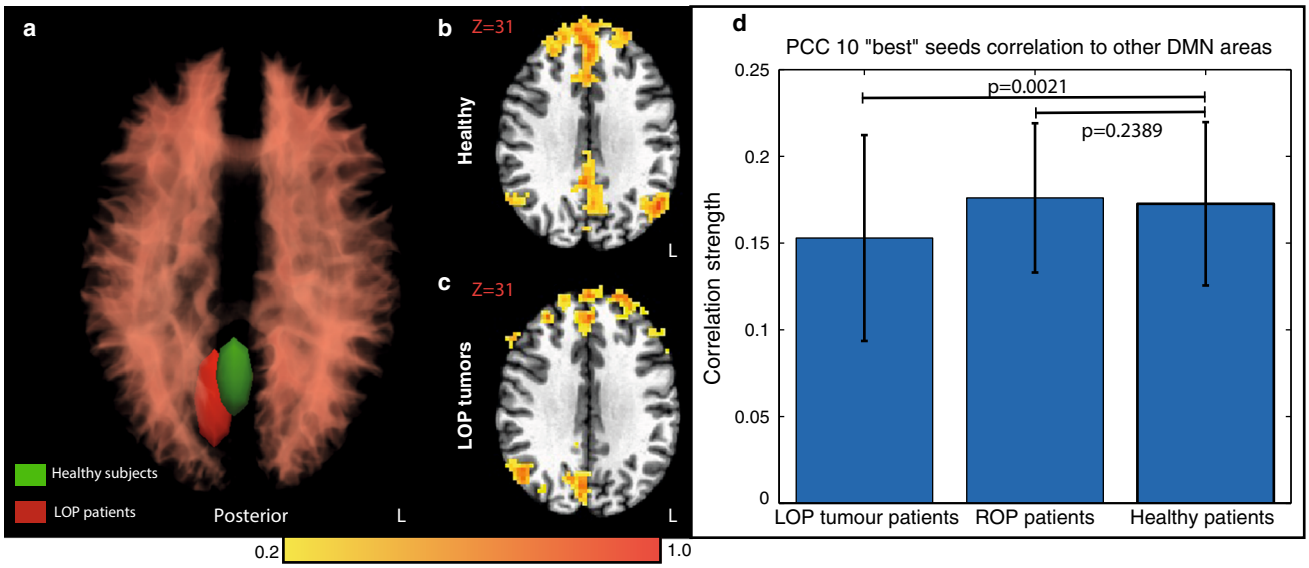

Fig. 2 **a** Average (x, y, z) coordinates in MNI space of the seed showing highest correlation to DMN areas (other than PCC and LAG). Radiuses of the ellipsoids represent standard deviations in x, y and z directions. **b** Average correlation maps using best seeds of healthy patients. **c** Average correlation maps using best seeds of LOP tumor affected patients. These results show deviation of PCC in LOP tumor patients. **d** Average correlation of PCC node seeds to other DMN nodes. The PCC node seeds were found by first placing 382 seeds in various areas of the PCC/precuneous area, and taking the 10 seeds which showed highest correlation to other DMN areas. The error bars represent simple standard deviations

tumors also may have displaced PCC node location, although this effect was not large enough to cause differences in connectivity on ICA and dual regression. Moreover, the "best" PCC seeds in patients with ROP tumors did not show significantly decreased correlation to other DMN nodes when compared to healthy controls. These results suggest that DMN connectivity in the left side of the brain may be more sensitive to the presence of a tumor than in the right side of the brain. In turn, this may be due to the asymmetry in functional connectivity observed in the healthy brain [21–26]. Our findings agree with a previous study using seed-based analysis which found that tumors in the parietal lobe of the brain tend to have a larger effect on DMN connectivity than tumors in the frontal lobe [5], and other studies which reported decreased DMN connectivity related to tumors [4, 20].

Our results also show that tumors in the cerebellum are associated with unilaterally decreased DMN connectivity at the left mPFC. This observation is sensible, as tracer studies have found fronto-cerebellar tracts that link the frontal lobe to the cerebellum [27, 28]. Moreover, recent findings have shown that the cerebellum may have a role in the DMN [29, 30]. As explained earlier, anatomy distortion cannot be held accountable for this result because the cerebellum and the mPFC are distant structures.

Interestingly, the effects we found on the default mode network were independent of tumor size, and histological type. Surprisingly, they were also unrelated to the pathophysiological nature of tumor growth. Indeed, we had assumed that infiltrative intra-axial tumors such as gliomas would have a more disruptive effect than extra-axial tumors or non-infiltrative tumor such as metastases. This

Table 3 Summary of results

Tumour parameter being studied	Statistical analysis	Results
Histological type of tumours	SBA and ANOVA	No significant difference between different histological types of tumours ($p = 0.4911$)
Tumour size	Linear regression	Tumour size was not a significant predictor of DMN overall connectivity, as defined previously ($p = 0.7199$)
Anatomical position of tumours	SBA and ANOVA	No significant difference between tumours of different position ($p = 0.1179$)
Anatomical position of tumours	ICA, dual regression and multi-seed	Tumours at left temporal lobe, left occipito-parietal lobe and at cerebellum cause significant decreases in DMN at various node locations. LOP tumours also displaced PCC in tumour patients. Effect of LOP tumours at PCC connectivity persisted after accounting for this anatomy distortion
Intracranial compartment of tumours	SBA and ANOVA	No significant difference between intraaxial and extraaxial tumours ($p = 0.7352$)
Invasiveness of tumours	SBA and ANOVA	No significant difference between infiltrative and non infiltrative tumours ($p = 0.4029$)

finding therefore suggests that the effects we have observed were entirely related to localization and direct mass effect exerted by the tumor. However, the lack of significant results could also be due to improper seed placement, as this part of the study was done in a "blind" fashion. There was not enough data to pool patients based on both tumor location and tumor histological/pathological type. Further investigation is necessary.

As a whole, the default mode network seems to be fairly robust and resistant to tumors. The decreases in connectivity reported in this paper caused by left sided and cerebellar tumors were statistically significant, but very small in absolute magnitude (see cluster sizes in Table 2 and correlation scales in Fig. 2d). This result is particularly important and interesting, as it shows that the default mode network is a structure that survives large clinically significant lesions like tumors. This could point to some particular importance of the default mode network in brain function.

Acknowledgments The authors are grateful for the help given by Russell Butler in the writing of this paper.

Funding K.W. is supported by a Canada Research Chair in Neurovascular Coupling and the Natural Sciences and Engineering Council of Canada (NSERC). S.G. is supported by a research grant from the Faculty of Medicine and Health Sciences of Université de Sherbrooke.

References

1. Mevel K, Grassiot B, Chetelat G, Defer G, Desgranges B, Eustache F (2010) The default mode network: cognitive role and pathological disturbances. Rev Neurol 166:859–872. doi:10.1016/j.neurol.2010.01.008
2. Raichle ME, MacLeod AM, Snyder AZ, Powers WJ, Gusnard DA, Shulman GL (2001) A default mode of brain function. Proc Natl Acad Sci USA 98:676–682. doi:10.1073/pnas.98.2.676
3. Broyd SJ, Demanuele C, Debener S, Helps SK, James CJ, Sonuga-Barke EJ (2009) Default-mode brain dysfunction in mental disorders: a systematic review. Neurosci Biobehav Rev 33:279–296. doi:10.1016/j.neubiorev.2008.09.002
4. Maesawa S, Bagarinao E, Fujii M, Futamura M, Motomura K, Watanabe H, Mori D, Sobue G, Wakabayashi T (2015) Evaluation of resting state networks in patients with gliomas: connectivity changes in the unaffected side and its relation to cognitive function. PLoS ONE 10:e0118072. doi:10.1371/journal.pone.0118072
5. Harris RJ, Bookheimer SY, Cloughesy TF, Kim HJ, Pope WB, Lai A, Nghiemphu PL, Liau LM, Ellingson BM (2014) Altered functional connectivity of the default mode network in diffuse gliomas measured with pseudo-resting state fMRI. J Neurooncol 116:373–379. doi:10.1007/s11060-013-1304-2
6. Liu J, Qin W, Wang H, Zhang J, Xue R, Zhang X, Yu C (2014) Altered spontaneous activity in the default-mode network and cognitive decline in chronic subcortical stroke. J Neurol Sci 347:193–198. doi:10.1016/j.jns.2014.08.049
7. Dacosta-Aguayo R, Grana M, Iturria-Medina Y, Fernandez-Andujar M, Lopez-Cancio E, Caceres C, Bargallo N, Barrios M, Clemente I, Toran P, Fores R, Davalos A, Auer T, Mataro M (2015) Impairment of functional integration of the default mode network correlates with cognitive outcome at three months after stroke. Hum Brain Mapp 36:577–590. doi:10.1002/hbm.22648
8. Rorden C, Brett M (2000) Stereotaxic display of brain lesions. Behavioural neurology 12:191–200
9. Hafkemeijer A, van der Grond J, Rombouts SA (2012) Imaging the default mode network in aging and dementia. Biochim Biophys Acta 1822:431–441. doi:10.1016/j.bbadis.2011.07.008
10. Cox RW (1996) AFNI: software for analysis and visualization of functional magnetic resonance neuroimages. Comput Biomed Res Int J 29:162–173
11. Cox RW, Hyde JS (1997) Software tools for analysis and visualization of fMRI data. NMR Biomed 10:171–178

12. Murphy K, Birn RM, Bandettini PA (2013) Resting-state fMRI confounds and cleanup. NeuroImage 80:349–359. doi:10.1016/j.neuroimage.2013.04.001
13. Smith SM, Jenkinson M, Woolrich MW, Beckmann CF, Behrens TE, Johansen-Berg H, Bannister PR, De Luca M, Drobnjak I, Flitney DE, Niazy RK, Saunders J, Vickers J, Zhang Y, De Stefano N, Brady JM, Matthews PM (2004) Advances in functional and structural MR image analysis and implementation as FSL. NeuroImage 23(Suppl 1):S208–S219. doi:10.1016/j.neuroimage.2004.07.051
14. Dipasquale O, Griffanti L, Clerici M, Nemni R, Baselli G, Baglio F (2015) High-dimensional ICA analysis detects within-network functional connectivity damage of default-mode and sensory-motor networks in Alzheimer's disease. Front Hum Neurosci 9:43. doi:10.3389/fnhum.2015.00043
15. Shirer WR, Ryali S, Rykhlevskaia E, Menon V, Greicius MD (2012) Decoding subject-driven cognitive states with whole-brain connectivity patterns. Cereb Cortex 22:158–165. doi:10.1093/cercor/bhr099
16. Filippini N, MacIntosh BJ, Hough MG, Goodwin GM, Frisoni GB, Smith SM, Matthews PM, Beckmann CF, Mackay CE (2009) Distinct patterns of brain activity in young carriers of the APOE-epsilon4 allele. Proc Natl Acad Sci USA 106:7209–7214. doi:10.1073/pnas.0811879106
17. Smith SM (2012) The future of FMRI connectivity. NeuroImage 62:1257–1266. doi:10.1016/j.neuroimage.2012.01.022
18. Winkler AM, Ridgway GR, Webster MA, Smith SM, Nichols TE (2014) Permutation inference for the general linear model. NeuroImage 92:381–397. doi:10.1016/j.neuroimage.2014.01.060
19. Nichols TE, Holmes AP (2002) Nonparametric permutation tests for functional neuroimaging: a primer with examples. Hum Brain Mapp 15:1–25
20. Esposito R, Mattei PA, Briganti C, Romani GL, Tartaro A, Caulo M (2012) Modifications of default-mode network connectivity in patients with cerebral glioma. PLoS ONE 7:e40231. doi:10.1371/journal.pone.0040231
21. Ribolsi M, Daskalakis ZJ, Siracusano A, Koch G (2014) Abnormal asymmetry of brain connectivity in schizophrenia. Front Hum Neurosci 8:1010. doi:10.3389/fnhum.2014.01010
22. Jalili M (2014) Hemispheric asymmetry of electroencephalography-based functional brain networks. NeuroReport 25:1266–1271. doi:10.1097/WNR.0000000000000256
23. Thatcher RW, Biver CJ, North D (2007) Spatial-temporal current source correlations and cortical connectivity. Clin EEG Neurosci 38:35–48
24. Tucker DM, Roth DL, Bair TB (1986) Functional connections among cortical regions: topography of EEG coherence. Electroencephalogr Clin Neurophysiol 63:242–250
25. Medvedev AV (2014) Does the resting state connectivity have hemispheric asymmetry? A near-infrared spectroscopy study. NeuroImage 85(Pt 1):400–407. doi:10.1016/j.neuroimage.2013.05.092
26. Yan H, Zuo XN, Wang D, Wang J, Zhu C, Milham MP, Zhang D, Zang Y (2009) Hemispheric asymmetry in cognitive division of anterior cingulate cortex: a resting-state functional connectivity study. NeuroImage 47:1579–1589. doi:10.1016/j.neuroimage.2009.05.080
27. Middleton FA, Strick PL (2001) Cerebellar projections to the prefrontal cortex of the primate. J Neurosci 21:700–712
28. Middleton FA, Strick PL (1994) Anatomical evidence for cerebellar and basal ganglia involvement in higher cognitive function. Science 266:458–461
29. Habas C, Kamdar N, Nguyen D, Prater K, Beckmann CF, Menon V, Greicius MD (2009) Distinct cerebellar contributions to intrinsic connectivity networks. J Neurosci 29:8586–8594. doi:10.1523/JNEUROSCI.1868-09.2009
30. Krienen FM, Buckner RL (2009) Segregated fronto-cerebellar circuits revealed by intrinsic functional connectivity. Cereb Cortex 19:2485–2497. doi:10.1093/cercor/bhp135

DISCUSSION

Our results confirm what has already been found in the literature and further elucidate how tumour location affects DMN connectivity. Similarly to the other groups which have studied the DMN in brain tumour patients (Esposito et al., 2012; Harris et al., 2014; Maesawa et al., 2015), we found that DMN connectivity was decreased in patients with brain tumours.

The main novel finding of this study was that tumours located in the left occipito-parietal lobe, left temporal lobe and the cerebellum had statistically significant effects on the default mode network, whereas all other sub-groups of tumour locations did not. It is interesting to notice that tumours located in the left portions of the brain had significant effects on DMN connectivity but the right sided counter parts did not. The DMN's greater fragility to tumours on one side of the brain may indicate that it is itself lateralised to some extent. In fact, it is possible that the act of not thinking or being in a "resting state" is to some extent a verbal exercise, as the participant being scanned might be actively telling himself "not to think", which would consequently engage the left hemisphere more than the right. Some studies have demonstrated some level of lateralisation of resting state networks including left lateralization of the DMN (Agcaoglu, Miller, Mayer, Hugdahl, & Calhoun, 2015).

On the other hand, comparison of the tumour distribution maps of left and right sided occipito-parietal lobe tumours (figure 1 of article 1) demonstrates that these tumours were not symmetrically distributed about the mid sagittal plane. In other words, the LOP tumours are not precisely in the same location in the left hemisphere as the ROP tumours are in the right hemisphere. This can be seen in figure 1 of article 1, which shows that the LOP tumours are closer to the midline than the ROP tumours. Thus, the greater effect of LOP tumours on the DMN may be due to their greater proximity to the PCC, which is a structure on the midline of the brain. Not only is the PCC an element of the DMN, it is also an important hub in the brain (Heuvel & Sporns, 2013); in other words, the PCC is functionally connected to a large number of regions in the brain. Tumours located nearer the PCC could be expected to have a larger effect on the DMN because of its importance in brain connectivity.

Negative results

Several interesting conclusions can also be drawn from the negative results of this study. In fact, we found that several tumour parameters, such as histology, compartment location and size, did not have an effect on the strength of the default mode network.

Tumour histology does not influence the DMN

First, it was shown that the histological type of a tumour does not have an impact on the strength of the DMN. This is a very surprising result, as we expected diffusely infiltrating tumours like gliomas to have a much larger effect on the default mode network than non-infiltrating tumours such as metastases and meningiomas. Our reason for believing this was primarily because infiltrating tumours such as gliomas have been shown to migrate along anatomical white matter tracts (Claes et al., 2007). Glioma cells could damage these white matter tracts through secretion of MMPs and other enzymes (Agnihotri et al., 2013; Rao, 2003), and thus decrease functional connectivity.

Moreover, glioma cells also migrate along blood vessels (Claes et al., 2007). The fMRI signal depends on the deoxyhemoglobin to oxyhemoglobin ratio in tissue, which itself is highly dependent on the underlying vasculature of the tissue.. It is thus surprising that migrating tumour cells had no impact on the regional fMRI signal, at least at the spatial resolution of our experiment. It is still plausible that migrating glioma cells may cause changes in microvasculature not detectable with conventional fMRI.

We did an additional analysis not described in article 1 to evaluate the effect gliomas may have on the fMRI signal. Briefly, we performed projection pursuit to see if there was any significant difference between the fMRI signal of voxels near the glioma and voxels far away from the glioma. Projection pursuit is a mathematical method that attempts to find a vector such that projecting two groups of data (the two groups of voxels) yields the largest difference between those two groups. For example, if the difference was that fMRI voxels near the glioma had a much larger signal at the 0.1 Hz frequency, then projection pursuit would yield a vector which represented a sinusoidal function with a 0.1 Hz frequency.

However, our projection pursuit did not yield a vector which showed a significant difference between the two groups of voxels. In other words, we could not find any significant difference in the fMRI signal of voxels near and far away from the glioma tumours. It is important to note however that the optimization problem in projection is very difficult and a significant limitation to this mathematical method.

Tumour compartment location does not influence the DMN

We showed that there was no difference in DMN connectivity between patients with intra-axial and extra-axial tumours. This is also surprising, as we expected intra-axial tumours to have a larger effect on connectivity. Since extra-axial tumours are not in the brain tissue itself, they do not have a direct effect on neuronal architecture, at least not to the same extent as intra-axial tumours. Rather, extra-axial tumours especially exert a compression effect on the underlying brain. Consequently, we hypothesized that extra-axial tumours would have a less extreme effect on the default mode network.

Tumour size does not influence the DMN

Size did not influence the tumours effect on the DMN. We expected larger tumours to exert greater compression effects on adjacent structures and cause greater distortions in anatomy which would lead to a larger effect on the DMN. Our inability to find this result is likely due to limitations of seed-based analysis and our sample size.

The DMN is fairly robust to lesions such as tumours

Finally, although we did find statistically significant differences in DMN connectivity between healthy and brain tumour patients, it is important to note that these differences were very small in absolute magnitude. This is appreciable in table 2 of article 1 and figure 2d of article 1. Table 2 shows that the clusters of significantly different voxels were very small, and figure 2d shows that the difference in correlation strength was also very small.

This suggests that the DMN is quite robust to surgical lesions like brain tumours, at least when compared to the results found in other pathologies, such as dementia or depression, where researchers have demonstrated very large differences in DMN connectivity (Andreescu et al., 2013; Li et al., 2013; Liston et al., 2014; Mevel et al., 2011). This is very interesting, as surgical lesions like brain tumours have an especially large effect on the structural integrity of the brain and tend to be more localised insults. Diseases like Alzhemier's and depression are widespread cerebral lesions, and are more neurochemical in nature: Alzheimer's being due to amyloid plaque depositions and depression due to lack of catecholamines and serotonin in the brain.

This provides some valuable insight as to what the DMN is: it seems to be more a function of the global brain state than it is of structural integrity. This result is surprisingly like what has been found in neurophysiological studies investigating correlated activity across neurons. In fact, studies have demonstrated that the extent of noise correlations across neurons seems to be related to the global brain state (Ecker et al., 2014). Noise correlations are the correlations of the trial to trial responses of different neurons, and they may have similar properties to networks detected with fMRI.

Strengths of the study

Use of several different techniques of extracting networks from fMRI

Unlike other studies, we used both seed based analysis and independent component analysis (in addition to multi-seed) on our data.

We believe the two methods are complimentary in the information they provide. SBA is model dependent and allowed us to evaluate whether overall DMN connectivity was increased/decreased in brain tumour patients. ICA is model independent and allowed us to build maps which showed where such increases/decreases were present.

Development and use of a novel rsfMRI techniques

Other studies evaluating the default mode network (and other networks) in brain tumour patients do not consider the effect that tumours can have on anatomy. With the multi-seed technique, we explicitly model this effect. The multi-seed method allows us to perform traditional SBA while not assuming the position of the PCC node.

Without multi-seed, it is difficult to evaluate whether the results in figure 1 of article 1 are due to PCC displacement or a genuine decrease in DMN connectivity. In the case of LOP tumours, it is easy to imagine that the PCC could be displaced by the tumours, and a simple misalignment of the PCC nodes would lead to a significant difference on voxel to voxel statistical comparisons. However, if there is a displacement of the PCC, the multi-seed technique will catch it as it does not assume a fixed coordinate location for the PCC; it allows the PCC node to vary from patient to patient. As it turns out, the LOP tumours did displace the PCC node, as can be seen from figure 2a of article 1, but that even when this displacement is taken into account, the decrease in DMN connectivity is still statistically significant. Previous studies investigating the effect of tumours on functional networks do not appropriately consider this effect.

Limitations of the study

Sample size

The main limitation of this study was the small sample size. We only had 73 patients enrolled in our study. Although this would be sufficient to blindly compare brain tumour patients to healthy controls (of which we had 23), we wanted to evaluate the effect of factors such as tumour histology and location. Properly controlling for both factors leads to groups with very small sample sizes, as can be seen in table 1 of article 1. These sub groups are far too small for meaningful statistical testing.

Diversity of brain tumours

Although our sample had a large variety of brain tumours, it was nonetheless very saturated with glioma patients (40/73). By comparison, there were only 12 metastases and 8 meningiomas (see table 1 of article 1). This may in part explain the lack of significant differences between histological groups found in the study: the study may have lacked the statistical power to resolve differences between such small groups.

Since the sample was largely saturated in gliomas, it is possible that the differences shown in figure 1 of article 1 were solely driven by the gliomas. This would confirm many of our suspicions prior to commencing the study.

Limitations of existing software

As was described in the article, registration of brain images with certain tumors to the MNI template was inadequate. Figure 13 shows an example of registration distortion: after registration to MNI template (right), the resulting brains are clearly distorted and inadequate for analysis. The failure of this brain to register is likely because of its massive deformities (brain tumour, hydrocephaly and loss of a large quantity of brain tissue). The registration algorithms such as in AFNI, FSL and SPM have been developed and validated in healthy brains and they are not adapted to images with brain tumors. If further fMRI studies are to be done in patients with brain tumours, better registration methods will have to be developed.

For linear registrations, which were used in this study, one potential solution would be to register non-tumour affected portions of the brain to the MNI atlas. In linear registration, a single transformation matrix is applied evenly to all portions of the brain. Registering only non-tumour portions of the brain would potentially dodge areas of anatomical distortion, and the resulting transformation matrix could be applied to the entire brain, including distorted regions. Testing of this method of registration is currently underway and may be subject to future publication.

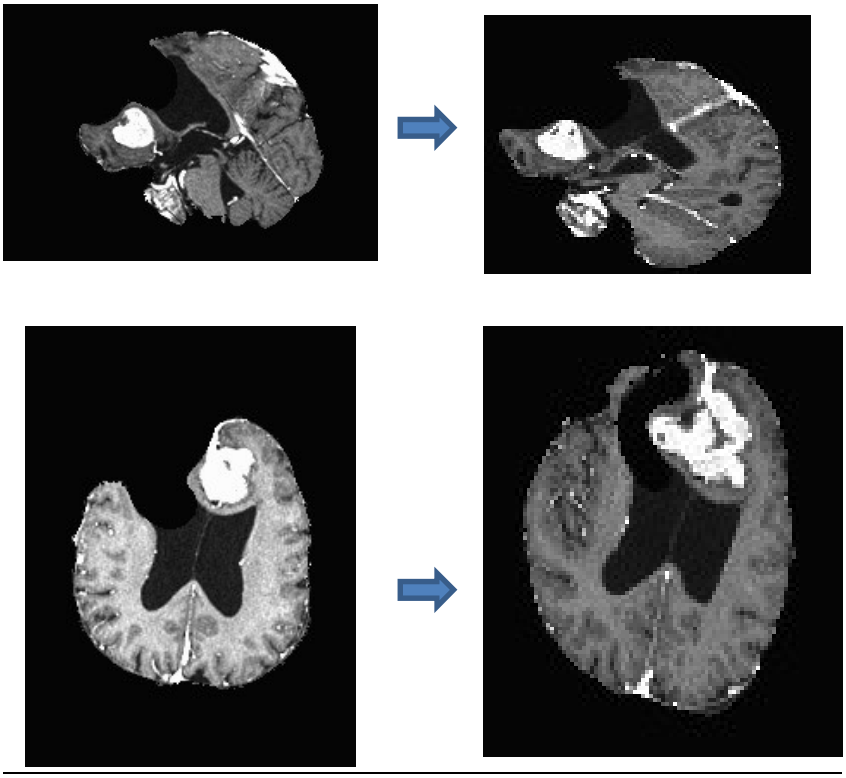

Figure 12 : Failure of registration methods

The images resulting from registering to the MNI template are grossly distorted (original images on left, registered images on right).

Limitations of seed based analysis

The largest weakness of seed based analysis (which was used to evaluate the effect of tumour histology, intracranial compartment and tumour size on the DMN's strength) is that this modality does not model the effects that the tumours may have on DMN node locations. If seed based analysis is done blindly, then seeds may accidently be placed directly in tumours, which would be clearly inadequate for DMN evaluation.

Moreover, even in the healthy brain, improper seed placement has been found to be one of the most important causes of study to study variability (Smith et al., 2011) . The weakness of seed based analysis could explain the lack of difference found when comparing tumours based on histological type.

Limitations of the multi-seed approach

Although the multi-seed was able to model the possible variability of a single DMN node location (as is shown in figure 2 of article 1), it assumes that each tumour only affects the nearest DMN node. However, brain tumours cause significant distortions of brain anatomy which likely affect all nodes of the brain at the same time.

Studying resting state networks in brain tumour patients thus requires a method of extracting these networks without making any assumptions about node locations. Individual subject ICA makes no assumption on the location of the network nodes, but there is no reasonable way of finding corresponding components across patients, which precludes groups comparisons.

Our group has attempted to develop a method consistent across all patients as is SBA and which adequately corrects for the entire impact of brain tumours on anatomy. This method involves first identifying regions which are susceptible of containing the default mode network: this is done by dilating traditional mask of the DMN. Within this dilated DMN mask, correlation coefficients are computed between each voxel and each other voxel, creating a large connectivity matrix. Then, the DMN mask is parcellated into two sub-masks using a standard graph parcellation algorithm. The algorithm parcellating the mask attempts to iteratively maximise the difference in connection density between the two sub-masks. The connection density of each sub-mask is the sum of unique values of the sub-mask's correlation matrix divided by the number of voxels within the sub-mask. Equation 1 demonstrates this mathematically.

$$\text{Parcellation fitness} = \sum_{i \neq j} \frac{(c_{ij})_A}{n_A} - \sum_{i \neq j} \frac{(c_{ij})_B}{n_B} \qquad \textbf{Equation 1}$$

Equation maximized by the parcellating algorithm. "c_{ij}" is the correlation score of the fMRI signals of voxel "i" and voxel "j". n_A is the number of voxels within submasks A.

Once equation 1 is optimised, the sub-mask with the higher connection density is the DMN: it represents the regions in the dilated DMN mask which are highly correlated to each

other, which is the DMN by definition on rsfMRI. This method, in our opinion, adequately models potential impacts brain tumours may have on the DMN; initially dilating the mask permits the algorithm to iteratively probe voxels which are not traditionally DMN related. Figure 14 demonstrates an example of this technique.

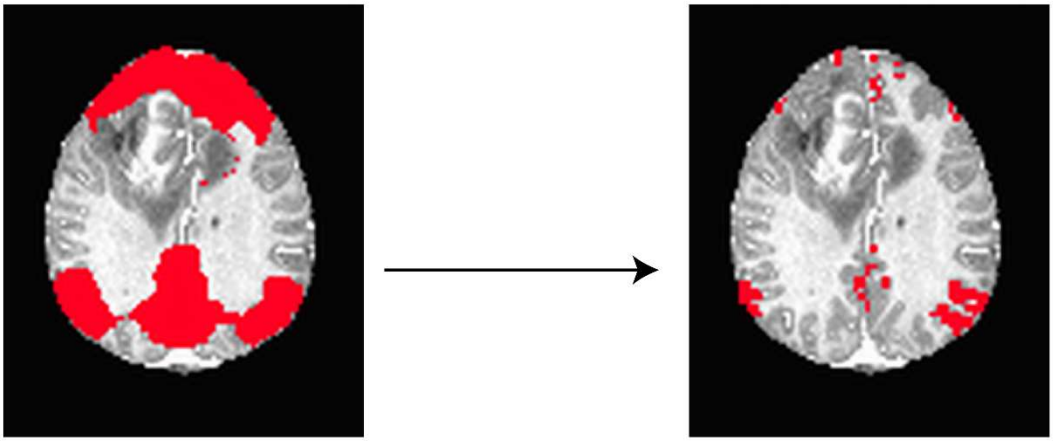

Figure 13 : Graph parcellation technique for extracting the DMN

Figure demonstrating the graph parcellation technique. The algorithm searches for voxels within the dilated DMN mask which are highly correlated to each other.

Patient movement

A limitation existing in all studies of patients with pathology is the bias brought by movement within the scanner. In fact, it has been shown that simple head motion during an fMRI scan can lead to differences in DMN connectivity (Van Dijk, Sabuncu, & Buckner, 2012). Visual examination of the fMRI scans suggested that there were non-trivial amounts of head motion in both the brain tumour and aging subjects. Although the effect of this motion was minimised with the appropriate image processing techniques, there is some concern that some of the differences (or lack of differences) observed in the study may have been due to different amounts of movement among the groups.

Non-automated portions of the analysis

Certain parts of the analysis of the patients with brain tumours required direct manual processing of the data. For example, the segmentation of the tumours in each individual had to be done manually. Since it is impossible for a human operator to segment each tumour in precisely the same way, this likely added some bias to the study's results. Ideally, segmentation would be done by an automated software which would perform the exact same procedure on all subjects.

Although this was not the primary goal of the study, we did attempt to find methods of automatically segmenting the brain tumours. Since the acquired images were T1 gadolinium enhanced, the most conceptually simple method of segmenting brain tumours would be to threshold the voxel intensity values. Since tumours capture gadolinium, they will have much higher intensity than surrounding tissue.

Two primary difficulties exist with this approach. First, there are structures other than the brain tumours which are enhanced with gadolinium, notably the vessels. Also, there is no easy way of choosing which threshold to use to segment the tumour exactly.

Our method of tumour segmentation is one step more sophisticated than simply thresholding the intensity values. Our method models tumours as being variation of normal brain tissue. To segment a tumour in a patient brain, that patient's brain is compared to the rest of the database of brain tumours. This is done with voxel by voxel z-tests: the intensity value at each voxel is compared to the mean of the rest of the tumour brains. Voxels which are largely different from the mean will have large Z-scores. The tumour can then be segmented by thresholding the Z-scores.

This method, of course, also suffers from the problem where there is no easy way of choosing which threshold to use for each brain tumour. Modern tumour segmentation approaches use much more involved algorithms than what has been described above. For example, some of these algorithms involve machine learning and attempting to classify pixels

as either tumour or non-tumour. Although our segmentation technique does not outperform these more involved methods, and is far more primitive as it only involves thresholding, we believe our approach of modelling brain tumours as being variations from normal brain tissue is novel.

Selection bias

All the patients chosen in the study were from the CHUS Fleurimont. Since Fleurimont is a tertiary reference center for cases of gliomas, it is possible that particularly severe cases of gliomas were over-represented in the study.

Future directions

Brain tumour research

This project demonstrated the effects that tumours can have on resting state connectivity. It demonstrated how tumours located in certain parts of the brain have a larger effect on functional connectivity. It was found that tumours near the PCC, which is a hub important for brain function (Heuvel & Sporns, 2013), have a larger effect on DMN connectivity than other tumours.

The findings of this study fit within the larger goal of developing fMRI as a diagnostic and prognostic tool in patients with brain tumours.. However, in order for fMRI to gain a role in the clinical management of brain tumours, much research is yet to be done.

First, there is a dire necessity to develop fMRI analysis tools which are validated in patients with cerebral pathologies. Unfortunately, many of the contemporary methods are developed and refined with healthy brains and do not generalise well to pathological brains. This problem becomes very clear in patients with brain tumours, as these patients have very severe distortions in cerebral anatomy which undermine many traditional rsfMRI methods of analysis. Limitations of linear registration methods and of connectivity analysis methods

(such as seed based analysis) were highlighted previously. We have done some work in rectifying this, with the development of the multi-seed approach. Moreover, we have also suggested a graph parcellation based method for finding networks in the brain, and a possible way of registering brains with surgical lesions that is less susceptible to failure. Developing automated techniques of tumour segmentation would also be very helpful to doing larger studies with more patients.

Second, validating fMRI as a prognostic tool would require a more comprehensive study which demonstrates the relationship between prognosis and the strength of certain networks. Such a study would need to acquire prognostic information, such as the number of days survived, metrics of autonomy (Karnofsky score), metrics of quality of life or any other score that quantifies the functional impact of the tumour.

Third, it may be interesting to investigate fMRI's potential as a diagnostic tool. Although developing fMRI for diagnosis was not the prime objective of the study, we did some preliminary work on the matter. We tested a machine learning algorithm's ability to determine the diagnoses of our brain tumour population when trained with connectivity data. In this analysis, the diagnostic labels were simply 'glioma' and 'not glioma'. The data fed into the algorithm was connectivity matrices built from each patient's fMRI data (procedure explained under *Graph theory* section of the introduction). The algorithm was trained with 20 patients and tested on the remaining 53. The results, however, were very disappointing, as the algorithm was correct only 50% of the time (equivalent to random chance). However, this disappointing result is very likely due to having an insufficient sample size.

Virtual biopsy

In addition to weak sample size, our previous analysis was also severely limited by the large complexity of the data. In fact, the previous analysis used connectivity matrices derived from the entire brain to determine diagnosis. However, we do not expect the global brain state to hold information relating to diagnosis, especially since our study demonstrated that the DMN was not different across various tumour histological types. As mentioned

earlier, gliomas are different from other tumours because they can migrate along vessels. Consequently, we expect that if diagnostic information exists in fMRI, it must be at the edge of the brain tumours, where the difference in migration patterns of the various types of brain tumours is manifested. To test this hypothesis, we developed an algorithm which grabs tissue at the exterior edge of each tumour (the algorithm grabs a virtual biopsy specimen).

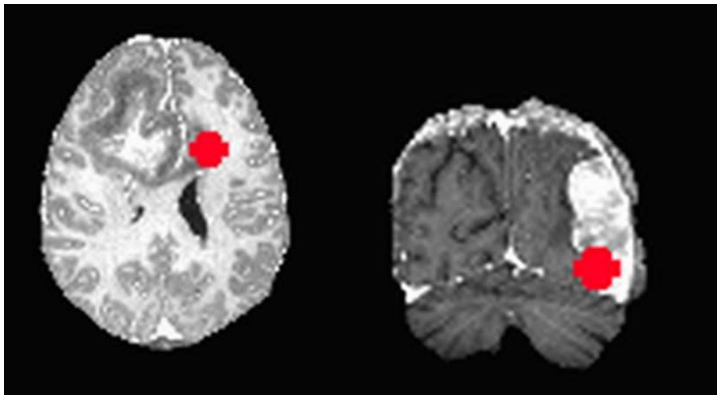

Figure 14 : Virtual biopsies taken from the brain

Figure 15 demonstrates how virtual biopsies were taken from the brains. Biopsy specimen were extracted from the edge of the brain tumour. It was hypothesized that different vascular properties in this region of the tumour might lead to different fMRI signals.

A correlation matrix is then computed for this biopsy specimen in each patient; we then tested if clustering these correlation matrices resulted in subgroups that were heavily associated with the diagnostic groups “glioma” and “not glioma”. We tested varying amounts of tissue sampling, but with our best result the clustering groups correctly predicted tumour diagnosis only 36 times (out of 64).

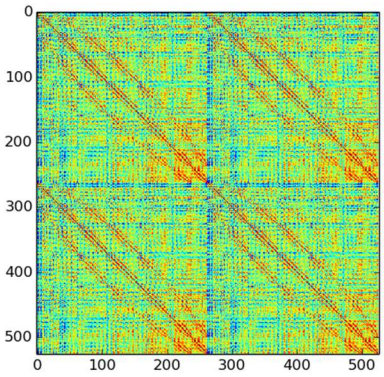

Figure 15 : Correlation matrix from a virtual biopsy

Figure demonstrates an example correlation matrix generated from the virtual biopsy technique. Correlation scores are computed from each voxel in the biopsy specimen to every other voxel, creating this matrix.

Multi-seed technique

Although the primary outcome of the research was the discovery of changes in the DMN in patients with brain tumours, the development of the multi-seed technique is an achievement itself worthy of some mention. We believe that this method of analysing fMRI data could be extended to other brain pathologies.

The multi-seed technique challenges the idea that DMN nodes are in fixed coordinate locations in all human brains, and proposes that these nodes should be allowed to vary to obtain the best representation of each patient's function networks. This is clearly important in patients with brain tumours, who have very obvious and discernable distortions of brain anatomy. However, this should also be true in various other cerebral conditions.

For example, aging patients have distortions of cerebral anatomy such as hydrocephaly and cortical atrophy which can confound traditional methods of connectivity analysis. Connectivity studies comparing aging to healthy brains have not considered this

effect. Some preliminary work we did on aging patients seems to suggest that anatomical changes in aging patients does somewhat bias connectivity research.

Similarly, several fMRI studies have been done investigating connectivity in patients with Alzheimer's disease and other dementias. These diseases are associated with well known changes of neuroanatomy, which could bias fMRI studies if not appropriately investigated. The multi-seed technique could be applied to these patients to evaluate the extent at which anatomical distortions affect fMRI connectivity values.

LISTE DES RÉFÉRENCES

Agcaoglu, O., Miller, R., Mayer, A. R., Hugdahl, K., & Calhoun, V. D. (2015). Lateralization of Resting State Networks and Relationship to Age and Gender. *NeuroImage*, (505), 310–325. http://doi.org/10.1016/j.neuroimage.2014.09.001.Lateralization

Agnihotri, S., Burrell, K. E., Wolf, A., Jalali, S., Hawkins, C., Rutka, J. T., & Zadeh, G. (2013). Glioblastoma , a Brief Review of History , Molecular Genetics , Animal Models and Novel Therapeutic Strategies. *Archivum Immunologiae et Therapiae Experimentalis*, *61*, 25–41. http://doi.org/10.1007/s00005-012-0203-0

Andreescu, C., Tudorascu, D. L., Butters, M. A., Tamburo, E., Patel, M., Price, J., … Aizenstein, H. (2013). Resting state functional connectivity and treatment response in late-life depression. *Psychiatry Research - Neuroimaging*, *214*(3), 313–321. http://doi.org/10.1016/j.pscychresns.2013.08.007

Andrew Kozel, F., Rao, U., Lu, H., Nakonezny, P. A., Grannemann, B., McGregor, T., … Trivedi, M. H. (2011). Functional connectivity of brain structures correlates with treatment outcome in major depressive disorder. *Frontiers in Psychiatry*, *2*(MAR), 1–7. http://doi.org/10.3389/fpsyt.2011.00007

Andrews-Hanna, J. R., Snyder, A. Z., Vincent, J. L., Lustig, C., Head, D., Raichle, M. E., & Buckner, R. L. (2007). Disruption of Large-Scale Brain Systems in Advanced Aging. *Neuron*, *56*(5), 924–935. http://doi.org/10.1016/j.neuron.2007.10.038

Beckmann, C., Mackay, C., Filippini, N., & Smith, S. (2009). Group comparison of resting-state FMRI data using multi-subject ICA and dual regression. *NeuroImage*, *47*, S148. http://doi.org/10.1016/S1053-8119(09)71511-3

Claes, A., Idema, A. J., & Wesseling, P. (2007). Diffuse glioma growth : a guerilla war. *Acta Neuropathologica*, *114*(5), 443–458. http://doi.org/10.1007/s00401-007-0293-7

Damoiseaux, J. S., Beckmann, C. F., Arigita, E. J. S., Barkhof, F., Scheltens, P., Stam, C. J., … Rombouts, S. A. R. B. (2008). Reduced resting-state brain activity in the “default network” in normal aging. *Cerebral Cortex*, *18*(8), 1856–1864. http://doi.org/10.1093/cercor/bhm207

Dennis, E. L., & Thompson, P. M. (2014). Functional brain connectivity using fMRI in aging and Alzheimer’s disease. *Neuropsychology Review*, *24*(1), 49–62.

http://doi.org/10.1007/s11065-014-9249-6

Ecker, A. S., Berens, P., Cotton, R. J., Subramaniyan, M., Denfield, G. H., Cadwell, C. R., … Tolias, A. S. (2014). State dependence of noise correlations in macaque primary visual cortex. *Neuron*, *82*(1), 235–248. http://doi.org/10.1016/j.neuron.2014.02.006

Esposito, R., Mattei, P. A., Briganti, C., Romani, G. L., Tartaro, A., & Caulo, M. (2012). Modifications of default-mode network connectivity in patients with cerebral glioma. *PLoS ONE*, *7*(7). http://doi.org/10.1371/journal.pone.0040231

Filippini, N., MacIntosh, B. J., Hough, M. G., Goodwin, G. M., Frisoni, G. B., Smith, S. M., … Mackay, C. E. (2009). Distinct patterns of brain activity in young carriers of the APOE-epsilon4 allele. *Pnas*, *106*(17), 7209–7214. http://doi.org/10.1073/pnas.0811879106

Fox, K. C. R., Spreng, R. N., Ellamil, M., Andrews-Hanna, J. R., & Christoff, K. (2015). The wandering brain: Meta-analysis of functional neuroimaging studies of mind-wandering and related spontaneous thought processes. *NeuroImage*, *111*, 611–621. http://doi.org/10.1016/j.neuroimage.2015.02.039

Fox, P. T., & Raichle, M. E. (1986). Focal physiological uncoupling of cerebral blood flow and oxidative metabolism during somatosensory stimulation in human subjects. *Proceedings of the National Academy of Sciences of the United States of America*, *83*(February 1986), 1140–4. http://doi.org/10.1073/pnas.83.4.1140

Fox, P. T., Raichle, M. E., Mintun, M. A., & Dence, C. (1988). Nonoxidative glucose consumption during focal physiologic neural activity. *Science (New York, N.Y.)*, *241*(4864), 462–464. http://doi.org/10.1126/science.3260686

Ghumman, S., Fortin, D., Noel-Lamy, M., Cunnane, S. C., & Whittingstall, K. (2016). Exploratory study of the effect of brain tumors on the default mode network. *Journal of Neuro-Oncology*, *128*(3), 437–444. http://doi.org/10.1007/s11060-016-2129-6

Gore, J. C. (2003). Principles and practice of functional MRI of the human brain. *Journal of Clinical Investigation*, *112*(1), 4–9. http://doi.org/10.1172/JCI200319010.Conventional

Hafkemeijer, A., van der Grond, J., & Rombouts, S. A. (2012). Imaging the default mode network in aging and dementia. *Biochim Biophys Acta*, *1822*(3), 431–441. http://doi.org/10.1016/j.bbadis.2011.07.008

Harris, R. J., Bookheimer, S. Y., Cloughesy, T. F., Kim, H. J., Pope, W. B., Lai, A., …

Ellingson, B. M. (2014). Altered functional connectivity of the default mode network in diffuse gliomas measured with pseudo-resting state fMRI. *Journal of Neuro-Oncology*, *116*(2), 373–379. http://doi.org/10.1007/s11060-013-1304-2

Heuvel, M. P. Van Den, & Sporns, O. (2013). Network hubs in the human brain. *Trends in Cognitive Sciences*, *17*(12), 683–696. http://doi.org/10.1016/j.tics.2013.09.012

Iadecola, C. (2004). Neurovascular regulation in the normal brain and in Alzheimer's disease. *Nature Reviews Neuroscience*, *5*(5), 347–360. http://doi.org/10.1038/nrn1387

Iadecola, C., & Nedergaard, M. (2007). Glial regulation of the cerebral microvasculature. *Nature Neuroscience*, *10*(11), 1369–1376. http://doi.org/10.1038/nn2003

Johnson, D. R., Ma, D. J., Buckner, J. C., & Hammack, J. E. (2012). Conditional Probability of Long-Term Survival in Glioblastoma. *Cancer*, *118*(22). http://doi.org/10.1002/cncr.27590

Koch, W., Teipel, S., Mueller, S., Buerger, K., Bokde, A. L. W., Hampel, H., … Meindl, T. (2010). Effects of aging on default mode network activity in resting state fMRI: Does the method of analysis matter? *NeuroImage*, *51*(1), 280–287. http://doi.org/10.1016/j.neuroimage.2009.12.008

Lang, E. W., Tomé, A. M., Keck, I. R., Gorriz-Saez, J. M., & Puntonet, C. G. (2012). Brain connectivity analysis: A short survey. *Computational Intelligence and Neuroscience*, *2012*(iii). http://doi.org/10.1155/2012/412512

Li, B., Liu, L., Friston, K. J., Shen, H., Wang, L., Zeng, L. L., & Hu, D. (2013). A treatment-resistant default mode subnetwork in major depression. *Biological Psychiatry*, *74*(1), 48–54. http://doi.org/10.1016/j.biopsych.2012.11.007

Liston, C., Chen, A. C., Zebley, B. D., Drysdale, A. T., Gordon, R., Leuchter, B., … Dubin, M. J. (2014). Default mode network mechanisms of transcranial magnetic stimulation in depression. *Biological Psychiatry*, *76*(7), 517–526. http://doi.org/10.1016/j.biopsych.2014.01.023

Louis, D. N., Perry, A., Reifenberger, G., Deimling, A. Von, Figarella, D., Webster, B., … Ellison, D. W. (2016). The 2016 World Health Organization Classification of Tumors of the Central Nervous System : a summary. *Acta Neuropathologica*, *131*(6), 803–820. http://doi.org/10.1007/s00401-016-1545-1

Maesawa, S., Bagarinao, E., Fujii, M., Futamura, M., Motomura, K., Watanabe, H., …

Wakabayashi, T. (2015). Evaluation of resting state networks in patients with gliomas: Connectivity changes in the unaffected side and its relation to cognitive function. *PLoS ONE*, *10*(2), 1–13. http://doi.org/10.1371/journal.pone.0118072

Mevel, K., Ch&#233, Telat, G., l, Eustache, F., Desgranges, B., & atrice. (2011). The Default Mode Network in Healthy Aging and Alzheimer's Disease. *International Journal of Alzheimer's Disease*, *2011*, e535816. http://doi.org/10.4061/2011/535816

Mulders, P. C., van Eijndhoven, P. F., Schene, A. H., Beckmann, C. F., & Tendolkar, I. (2015). Resting-state functional connectivity in major depressive disorder: A review. *Neuroscience and Biobehavioral Reviews*, *56*, 330–344. http://doi.org/10.1016/j.neubiorev.2015.07.014

Ogawa, S., Lee, T. M., Kay, A. R., & Tank, D. W. (1990). Brain magnetic resonance imaging with contrast dependent on blood oxygenation. *Proceedings of the National Academy of Sciences of the United States of America*, *87*(24), 9868–72. http://doi.org/10.1073/pnas.87.24.9868

Rao, J. S. (2003). Molecular Mechanisms of Glioma Invasiveness: The Role of Proteases. *Nature Reviews. Cancer*, *3*(July), 489–501. http://doi.org/10.1038/nrc1121

Salomons, T. V, Dunlop, K., Kennedy, S. H., Flint, A., Geraci, J., Giacobbe, P., & Downar, J. (2014). Resting-State Cortico-Thalamic-Striatal Connectivity Predicts Response to Dorsomedial Prefrontal rTMS in Major Depressive Disorder. *Neuropsychopharmacology*, *39*(2), 488–498. http://doi.org/10.1038/npp.2013.222

Scott, J., Rewcastle, N., Brasher, P., Fulton, D., MacKinnon, J., Hamilton, M., … Forsyth, P. (1999). Which glioblastoma multiforme patient will become a long-term survivor? A population-based study. *Annals of Neurology*, *46*(2), 183–8.

Smith, S. M., Miller, K. L., Salimi-khorshidi, G., Webster, M., Beckmann, C. F., Nichols, T. E., … Woolrich, M. W. (2011). Network modelling methods for FMRI. *NeuroImage*, *54*(2), 875–891. http://doi.org/10.1016/j.neuroimage.2010.08.063

Thakkar, J. P., Dolecek, T. A., Horbinski, C., Ostrom, Q. T., Lightner, D. D., Barnholtz-Sloan, J. S., & Villano, J. L. (2014). Epidemiologic and Molecular Prognostic Review of Glioblastoma. *Cancer Epidemiology*, *23*(10), 1985–1996. http://doi.org/10.1158/1055-9965.EPI-14-0275.Epidemiologic

Tuladhar, A. M., Snaphaan, L., Shumskaya, E., Rijpkema, M., Norris, D. G., & Leeuw, F.

De. (2013). Default Mode Network Connectivity in Stroke Patients. *PLoS ONE*, *8*(6). http://doi.org/10.1371/journal.pone.0066556

van den Heuvel, M. P., & Hulshoff Pol, H. E. (2010). Exploring the brain network: A review on resting-state fMRI functional connectivity. *European Neuropsychopharmacology*, *20*(8), 519–534. http://doi.org/10.1016/j.euroneuro.2010.03.008

Van Dijk, K. R. A., Sabuncu, M. R., & Buckner, R. L. (2012). The Influence of Head Motion on Intrinsic Functional Connectivity MRI. *NeuroImage*, *59*(1), 431–438. http://doi.org/10.1016/j.neuroimage.2011.07.044.The

Vigneau-roy, N., Bernier, M., Descoteaux, M., & Whittingstall, K. (2013). Regional Variations in Vascular Density Correlate With Resting-State and Task-Evoked Blood Oxygen Level-Dependent Signal Amplitude. *Human Brain Mapping*, *35*(5), 1906–1920. http://doi.org/10.1002/hbm.22301